HHS Public Access

Author manuscript

Neuroscience. Author manuscript; available in PMC 2019 November 21.

Published in final edited form as:

Neuroscience. 2018 November 21; 393: 236–257. doi:10.1016/j.neuroscience.2018.10.002.

Sex differences in the rat hippocampal opioid system after oxycodone conditioned place preference

James D. Ryan[#1,2], **Yan Zhou**[#3], **Natalina H. Contoreggi**[1], **Farah K. Bshesh**[4], **Jason D. Gray**[5], **Joshua F. Kogan**[5], **Konrad T. Ben**[3], **Bruce S. McEwen**[5,*], **Mary Jeanne Kreek**[3,*], and **Teresa A. Milner**[1,2,5,*]

[1]Feil Family Brain and Mind Research Institute, Weill Cornell Medicine, 407 East 61st Street, New York, NY 10065

[2]Weill Cornell Graduate School of Medical Sciences, Weill Cornell Medicine, 1300 York Ave, New York, NY 10065

[3]The Laboratory of the Biology of Addictive Diseases, The Rockefeller University, 1230 York Avenue, New York, NY 10065

[4]Weill Cornell Medicine in Qatar, Qatar Foundation, Education City, P.O. Box 24144 - Doha, Qatar

[5]Harold and Margaret Milliken Hatch Laboratory of Neuroendocrinology, The Rockefeller University, 1230 York Avenue, New York, NY 10065

[#] These authors contributed equally to this work.

Abstract

Although opioid addiction has risen dramatically, the role of gender in addiction has been difficult to elucidate. We previously found sex-dependent differences in the hippocampal opioid system of Sprague-Dawley rats that may promote associative learning relevant to drug abuse. The present studies show that although female and male rats acquired conditioned place preference (CPP) to the mu-opioid receptor (MOR) agonist oxycodone (3mg/kg, I.P.), hippocampal opioid circuits were differentially altered. In CA3, Leu-Enkephalin-containing mossy fibers had elevated levels in oxycodone CPP (Oxy) males comparable to those in females and sprouted in Oxy-females, suggesting different mechanisms for enhancing opioid sensitivity. Electron microscopy revealed that in Oxy-males delta opioid receptors (DORs) redistributed to mossy fiber-CA3 synapses in a manner resembling females that we previously showed is important for opioid-mediated long-term potentiation. Moreover, in Oxy-females DORs redistributed to CA3 pyramidal cell spines

Corresponding author: Teresa A. Milner, Ph.D., Feil Family Brain and Mind Research Institute, Weill Cornell Medicine, 407 East 61st Street, RM 307, New York, NY 10065 United States of America, Phone: (646) 962-8274, FAX: (646) 962-0535, tmilner@med.cornell.edu. Address correspondence to: jdr2003@med.cornell.edu or tmilner@med.cornell.edu.

[*]Co-Senior authors

Author Contributions: T.A.M., M.J.K. and B.S.M. designed research; J.D.R, Y.Z., N.H.C., F.K.B., J.D.G, J.F.K., K.T.B., T.A.M. performed research; J.D.R., N.H.C., F.K.B., T.A.M. analyzed data; J.D.R., Y.Z., N.H.C., J.D.G., T.A.M., B.S.M., M.J.K. wrote the paper.

Conflict of Interest: The authors declare no competing financial interests.

suggesting the potential for enhanced plasticity processes. In Saline-injected (Sal) females, dentate hilar parvalbumin-containing basket interneuron dendrites had fewer MORs, however, plasmalemmal and total MORs increased in Oxy-females. In dentate hilar GABAergic dendrites that contain neuropeptide Y, Sal-females compared to Sal-males had higher plasmalemmal DORs, and near-plasmalemmal DORs increased in Oxy-females. This redistribution of MORs and DORs within hilar interneurons in Oxy-females would potentially enhance disinhibition of granule cells via two different circuits. Together, these results indicate that oxycodone CPP induces sex-dependent redistributions of opioid receptors in hippocampal circuits in a manner facilitating opioid-associative learning processes and may help explain the increased susceptibility of females to opioid addiction acquisition and relapse.

Graphical Abstract:

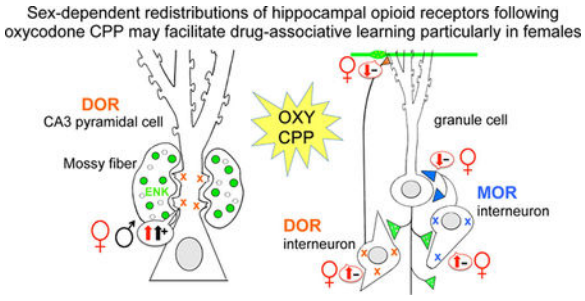

Keywords

Leu-Enkephalin; Delta opioid receptor; Mu opioid receptor; Electron microscopy; Drug addiction

INTRODUCTION

Opioid use and abuse has risen dramatically over the last two decades (Centers for disease control and prevention 2015). The role of gender in opioid addiction processes has been difficult to elucidate. In particular, separating biological effects from the impact of the environment, genetics and multidrug use is challenging in clinical data. However, evidence from rodent studies indicates that hormonal status likely plays a role in opioid addiction (Becker et al., 2017). For instance, cyclical fluctuations in circulating estrogen levels, corresponding to the human menstrual cycle and the rodent estrous cycle, have been shown to alter morphine sensitivity in women (Ribeiro-Dasilva et al., 2011) and patterns of heroin self-administration in rats (Lacy et al., 2016).

In both sexes, the transition from drug use to drug addiction critically depends on regions and neural circuits involved in associative memory formation and the encoding of motivational incentives (Koob and Volkow, 2010). The action of commonly abused opioid receptor agonists like oxycodone and morphine is in large part mediated by their effects on the regions that compose the mesolimbic reward circuit in addition to regions that either innervate or receive projections from canonical reward areas (Berke and Hyman, 2000; Hyman et al., 2006; Volkow et al., 2006). While neuroanatomical sex-dependent differences in mesolimbic reward circuit regions like the nucleus accumbens (Wissman et al., 2012) and

ventral tegmental area (Gillies et al., 2014) have been observed, hippocampal circuits that modulate contextual drug learning are also involved in addiction processes (Koob and Volkow, 2010).

Within the rodent hippocampus, opioid signaling in the CA3 subregion has been shown to play a critical role in spatial memory and in contextual associative learning (Meilandt et al., 2004; Kesner and Warthen, 2010). In CA3, the opioid peptide enkephalin is largely contained in the mossy fiber pathway and, to a lesser extent, the lateral perforant path [reviewed in (Drake et al., 2007)]. The mossy fiber pathway in the CA3 and hilus of the dentate gyrus (DG) overlaps Gamma-amino butyric acid (GABA) interneurons containing μ opioid receptors (MORs) and δ opioid receptors (DORs) [reviewed in (McEwen and Milner, 2017)]. Enkephalins and exogenous opiates such as morphine and oxycodone inhibit GABAergic interneurons via the activation of MORs and DORs, which consequently results in the disinhibition of CA3 pyramidal neurons and a subsequent change in their intrinsic excitability that promotes long-term potentiation [LTP; (Drake et al., 2007; Harte-Hargrove et al., 2015)]. Previous work from our laboratory has shown that the mossy fiber-CA3 pathway demonstrates decreased MOR-mediated basal transmission and exhibits a low-frequency DOR-mediated LTP in female rats in high estrogen states, but not in low estrogen states or in males (Harte-Hargrove et al., 2015). Moreover, our light and electron microscopic (EM) studies have revealed significant sex differences in the rat mossy fiber opioid system [reviewed in (McEwen and Milner, 2017)]. High estrogen state female rats compared to low estrogen state females and males have: 1) elevated levels of Leu^5-enkephalin (LEnk) in mossy fibers (Torres-Reveron et al., 2009b; Pierce et al., 2014); 2) greater densities of DORs in CA3 pyramidal cell spines contacted by mossy fibers (Williams et al., 2011a; Harte-Hargrove et al., 2015; Mazid et al., 2016); 3) elevated densities of DORs near the plasmalemma of GABAergic hilar interneurons (Mazid et al., 2016); and 4) greater densities of MORs on the plasmalemma of parvalbumin (PARV)-containing interneurons (Torres-Reveron et al., 2009a; Milner et al., 2013). Together these findings suggest that the opioid system in females is primed to promote excitation and contextual learning processes following opiate exposure.

The goal of this study was to investigate the effect of oxycodone conditioned place preference (CPP) on the levels of LEnk and the subcellular distribution and trafficking of MORs and DORs in neurons within the dorsal hippocampus of female and male Sprague Dawley rats. For this, light and EM immunocytochemical methods were used. We find that oxycodone CPP results in sex-dependent alterations within hippocampal opioid circuits that would facilitate drug-associated learning particularly in females.

EXPERIMENTAL PROCEDURES

Animals

Twenty-four adult male (~275–325 grams at the time of arrival) and adult female (~225–250 grams at the time of arrival) Sprague-Dawley rats (RGD Cat# 734476, RRID:RGD_734476) were used for all experiments described within this study. To minimize variability in the environment (including the vivarium and seasonal variability in phytoestrogen levels in the rat chow) as well as handling by different investigator, the present experiment was

performed on a single cohort of female and male rats was obtained from the vendor at the same time. Upon arrival in the animal facility, rats were single-housed in R20 rat cages (10.5 in x 19 in x 8 in; Ancare, Bellmore NY) with *ad libitum* food (PicoLab Rodent diet 20; LabDiet, St. Louis MO) and water in a room with a 12:12 light/dark cycle (lights on at 0600). All procedures were approved by the Rockefeller University and Weill Cornell Medicine Institutional Animal Care and Use Committees, and were compliant with the 2011 Eighth Edition of the NIH guidelines for the Care and Use of Laboratory Animals.

Handling and Estrous Cycle Determination

Handling can have significant effects on rodent cortisol levels (Deutsch-Feldman et al., 2015; Collins et al., 2016). Our previous experiments determined that gentle regular handling by the same investigators before experimenter-provided drug administration paradigms reduced corticosterone concentrations in adult male rats (Deutsch-Feldman et al., 2015). Thus, in the present experiment rats were handled by the same investigators (Y.Z. and K.T.B.) and subjected to behavioral testing between 9:00 am and 1:00 pm each day throughout the experiment. Following acclimation to the animal facilities for one week, rats were picked up and gently stroked for 3–5 minutes per day for five days prior to behavioral testing.

Previous studies have shown that regular estrous cycle monitoring of rodents using vaginal lavage or swabbing will attenuate associative memory behaviors including cocaine CPP (Walker et al., 2001; Walker et al., 2002; Van Kempen et al., 2014). Additionally, regular estrous cycling monitoring with vaginal lavage alone can induce a significant preference for side in the CPP apparatus (Walker et al., 2002). Given these caveats with estrous cycling and CPP behavior as well as the difficulty in mimicking this exact process in males, estrous cycle stage of female rats was only determined on the day of euthanasia in the present study. For this, vaginal smear cytology (Turner and Bagnara, 1971) was used after rats were deeply anesthetized and prior to aortic perfusion (described below). Consistent with our previous studies (Milner et al., 2013; Pierce et al., 2014; Mazid et al., 2016), estrous cycles were classified as proestrus (elevated estrogen levels, 0.5–1 day long), estrus (declining estrogen levels, 2–2.5 days long), or diestrus (low estrogen and progestin levels, 2–2.5 days long).

Oxycodone conditioned place preference

Rats were subjected to oxycodone CPP behavior in a procedure similar to our previous studies in mice (Zhang et al., 2016). Behavioral experiments on cohorts of rats were staggered over a period of 4 days between 9am and 1pm for all rats. The CPP apparatus (Med Associates Inc., Fairfax VT) consisted of three compartments (a white compartment, a black compartment, and a central gray compartment) separated by removable doors. During the test, locomotor activity and time spent in each compartment was monitored using infrared photobeams. A dose of 3 mg/kg (i.p.) oxycodone (Sigma-Aldrich #O1378) was chosen because it has been shown to induced 90–100% CPP in female rats in previous studies (Olmstead and Burns, 2005) and in both sexes in our pilot studies. Recent studies have demonstrated that female Sprague-Dawley rats have normal estrous cycles following self-administration of escalating doses of oxycodone (0.003, 0.01, 0.03, 0.1 and 0.3 mg/kg/infusion with up to 40 infusions per trial) in daily 1-hour trials over the course of 1 month

(Mavrikaki et al., 2017); the dose and duration of oxycodone in the present study was substantially lower than those in this study.

The CPP protocol followed a 14-day sequence: 1) preconditioning: During day 1, the compartment doors were removed and rats were allowed to freely explore the entire apparatus for 30 minutes. The results of preconditioning revealed a compartment bias dependent on sex (females preferred the black compartment and males preferred the white compartment); subsequently, we proceeded using a biased CPP design in which oxycodone administration occurred in the least-preferred side for that sex. 2) CPP training: On days 2 through 9 of CPP, the removable doors were added to the apparatus to separate compartments. There were a total of four training sessions, each two days long. On the first day of each session, rats were injected with oxycodone (3 mg/kg, i.p.) and then immediately placed in the non-preferred compartment for 30 minutes [a time point within the 3–5 hour half-life of oxycodone (Ordonez Gallego et al., 2007)]. On the second day of each session the rats were injected with saline and placed in the side opposite to where they were injected with oxycodone. The control rats were injected with saline on both days of each session. The rats were left undisturbed in their home cage prior to the CPP test. 3) CPP test: On day 14 (4 days following last injection), the doors separating the compartments were removed. The rats received no injections and were placed in the neutral, central gray compartment of the CPP apparatus. Their behavior was monitored for 30 minutes. The difference in percent of time spent in the drug-paired compartment vs. the drug-unpaired compartment was compared. Preconditioning levels were used to determine whether rats developed a preference for the oxycodone-associated side of the CPP apparatus.

Immunocytochemistry Procedures

Section Preparation—Euthanasia of cohorts of rats occurred between 9am and 1pm over a period of 4 days. The same investigators (J.D.G, J.D.K. and T.A.M.) performed all fixation procedures. Rats were deeply anesthetized with a mixture of ketamine (100 mg/kg) and xylazine (10 mg/kg) and perfused through the ascending aorta sequentially with: 1) 10–15 ml 0.9% saline, 2) 50 ml of 3.75% acrolein and 2% paraformaldehyde (PFA) in 0.1 M phosphate buffer (PB, pH = 7.4), and 3) 200 ml of 2% PFA in PB. Brains then were removed from the skull, cut into 5 mm coronal blocks, and post-fixed in 2% PFA in PB for 30 minutes before being transferred into PB. Sections (40 μM thick) through the hippocampus were cut using a vibrating microtome (Leica Microsystems, Buffalo Grove, IL) into 24-well plates containing PB. Sections were stored in a cryoprotectant solution (30% sucrose and 30% ethylene glycol in PB) at −20°C. For each immunocytochemical experiment, dorsal hippocampal [−3.5 to −4.2 mm from Bregma (Swanson, 1992)] sections were used. To rigorously control for variability in immunocytochemical processing and reagents, it is critical for tissues for quantitative light microscopic and EM immunocytochemical studies to be processed in one experiment (Pierce et al., 1999). Thus, to ensure identical labeling conditions between groups, the sections were processed together in single containers and coded with hole punches for each experiment. Sections were incubated in 1% sodium borohydride in PB for 30 minutes to neutralize reactive aldehydes (Milner et al., 2011) then rinsed 8–10 times in PB.

Antibody Characterization

DOR: A rabbit polyclonal antibody against amino acids 3–17 of DOR protein (Millipore Cat# AB1560, RRID:AB_90778) was used in this study. An extensive description of previous characterization studies can be found in Mazid et al. (2016). Briefly, the DOR AB1560 has been characterized in Western blots of lysates from rat brains and in NG108–15 cells, which endogenously express DORs (Barg et al., 1984; Persson et al., 2005; Saland et al., 2005) and in preadsorption controls on tissue sections (Olive et al., 1997). Moreover, no detectable labeling of this antibody is seen in Western blots of COS-7 cells [see Supplemental Fig. 1 in (Williams et al., 2011a)], which do not endogenously express DORs (Kieffer et al., 1992) as well as in the dorsal raphe of DOR knockout mice [see Supplemental Fig. 1 (Bie et al., 2010)]. Further, the greater DOR-immunoreactivity (DOR-ir) with AB1560 in interneurons compared to pyramidal cells in the rat hippocampus is consistent with DOR mRNA expression in this species (Mansour et al., 1994). Previous autoradiography experiments have described DOR binding sites in the rat hippocampus that corroborate the DOR-ir seen with this antibody (Crain et al., 1986; Gulya et al., 1986; Mansour et al., 1987; McLean et al., 1987).

The AB1560 antibody has been used in our previous light microscopic and EM studies (Commons and Milner, 1996; Williams et al., 2011b; Williams and Milner, 2011; Williams et al., 2011a; Mazid et al., 2016). DOR-ir in the rat hippocampus is sensitive to fixation, and thus yields the most intense labeling with 3.75% acrolein and 2% PFA fixed sections compared to 4% PFA fixed sections (Commons and Milner, 1997).

Enkephalin: A mouse monoclonal antibody to LEnk from Sera Labs (MAS 083p, clone NOCl, Lot P91G083; Crawley Down, UK) was used in this study. In immunoblots and adsorption controls, this antibody recognizes LEnk, and to a lesser extent dynorphin A and met-enkephalin, but not β-endorphin (Milner et al., 1989). This antibody has been used previously to immunolabel the rat and mouse hippocampal mossy fiber pathway (Commons and Milner, 1995; Torres-Reveron et al., 2008; Van Kempen et al., 2013; Pierce et al., 2014; Rogers et al., 2016).

GABA: A rat polyclonal antiserum selective against GABA-glutaraldehyde-hemocyanin conjugates was provided courtesy of Dr. A. Towle (formerly at Cornell University Medical College). The specificity of this antiserum was confirmed using preadsorption with GABA-bovine serum albumin (BSA), where it was found to eliminate immunoreactivity. However, preadsorption with unconjugated GABA or BSA conjugated to glutamate, β-alanine or taurine did not abolish immunoreactivity (Lauder et al., 1986). The overall immunoreactivity of this antiserum is found to be consistent with that of other GABA-specific antisera (Lauder et al., 1986). This antibody has been used in previous light and EM studies (Drake and Milner, 1999; Mazid et al., 2016).

MOR: A rabbit polyclonal antibody (Neuromics Cat# RA10104–150, RRID:AB_2156526) was used in this study. The antibody specifically recognizes a 15-amino acid sequence (residues 384–398) in the C-terminus of MOR1, but does not recognize the spliced variant MOR-1B-E or the cloned DOR (Arvidsson et al., 1995; Abbadie et al., 2000). The

specificity of this antibody has been demonstrated through Western blotting, adsorption controls, and omission controls in rat tissue (Arvidsson et al., 1995; Drake and Milner, 1999).

The high immunoreactivity of MOR in PARV-labeled dendrites seen in this study and in our previous studies (Torres-Reveron et al., 2009a; Milner et al., 2013) is corroborated by previous work showing high MOR mRNA expression within subsets of GABAergic cells in the hippocampus (Stumm et al., 2004). Our previous studies in rats revealed that MOR-ir is most commonly colocalized with PARV-ir and seldom with somatostatin which is contained in another subset of GABA cells (Drake and Milner, 2006).

PARV: A mouse monoclonal PARV antibody (Sigma-Aldrich Cat# P3088, RRID:AB_477329) was used in this study. This antibody has been previously identified by its ability to recognize PARV in brain tissue through radioimmunoassay and immunoblots (Celio et al., 1988; Celio, 1990).

Light Microscopic Immunocytochemistry

Experimental procedure: Hippocampal tissue sections were processed using previously described methods (Milner et al., 2011) to assess changes in the density of LEnk- and DOR-immunoreactivities. Briefly, tissue sections were rinsed in 0.1M Tris-buffered saline (TS; pH = 7.6) and then blocked in 0.5% BSA in TS for 30 minutes. Cohorts of sections were incubated in either mouse anti-LEnk (1:15,000 dilution) or rabbit anti-DOR (1:5000 dilution) antibody in 0.1% BSA and TS for 24 hours at room temperature (25°C) followed by an additional 24 hour incubation at 4°C. Triton X-100 (0.25%) was added to the LEnk antibody diluent. Next, sections were incubated in a 1:400 dilution of either biotinylated horse anti-mouse immunoglobulin (IgG; LEnk; Vector Laboratories Cat# BA-2001; RRID:AB_2336180) or donkey-anti-rabbit IgG (DOR; Jackson Immunoresearch Laboratories, Cat# 711–506-152, RRID:AB_2616595) for 30 minutes followed TS rinses. Sections then were incubated in avidin-biotin complex (ABC; Vectastain elite kit, Vector Laboratories, Burlingame, CA) at half the manufacturer's recommended dilution for 30 minutes. After washing in TS, tissue sections then were reacted in a 3,3'-diaminobenzidine (DAB; Sigma-Aldrich, St. Louis, MO) and 3% H_2O_2 in TS for 5–6 minutes. Tissue sections then were mounted on 1% gelatin-coated glass slides, dehydrated through an ascending series of ethanols, and coverslipped from xylene with DPX mounting media (Sigma-Aldrich).

Analysis 1: LEnk and DOR levels: Densitometric quantification for LEnk-immunoreactivity (LEnk-ir) and DOR-ir within the hippocampus was performed using previously described methods (Williams et al., 2011a; Pierce et al., 2014). Briefly, all slides first were coded for blind analysis. Images of the hippocampus on slide-mounted tissue sections were captured at 4x (except for LEnk-ir in stratum oriens (SO) which was captured at 10x) on a Nikon Eclipse 80i microscope using a Dage MTI CCD-72 camera and IP Lab software (Scanalytics IPLab, RRID:SCR_002775). ImageJ64 (ImageJ, RRID:SCR_003070) software was used to determine average pixel density within hippocampal regions of interest (ROI). For LEnk, pixel density was determined in seven ROIs within the hippocampus: the

crest, central region, and dorsal blade of the DG, stratum lucidum (SLu) of CA3 a, b and c and SO lateral to CA3a (Fig. 2A). For DOR, SO, SLu and stratum radiatum (SR) of CA3b were measured (Fig 5A). To control for variations in overall illumination levels between images and to compensate for background staining, the pixel density of a small region lacking labeling (LEnk: SR of CA1; DOR: white matter) was subtracted from ROI measurements. The accuracy of this technique with this hardware and software was corroborated by a strong linear correlation between average pixel density and actual transmittance by Pierce et al. (2014). In addition to density, the width of LEnk-labeling in SLu CA2/CA3a and CA3b was measured.

Analysis 2: DOR cell counts: The number of DOR cells was determined in the DG hilus using previously described methods (Williams et al 2011b). All DOR-labeled cells containing a nucleus were counted within the DG hilus. Using the granule cell layer and CA3 pyramidal cell layers as borders, the area of the hilus was measured using imageJ64 software. The number of cells per mm^2 was then calculated. The number of cells in the crest, central hilus and dorsal blade of the hilus was determined by randomly placing a 200 μm^2 rectangle over these regions using the granule cell layer as a guide.

Dual Labeling Electron Microscopic (EM) Immunocytochemistry

Experimental procedure: Tissue sections were dual labeled for either DOR and GABA or MOR and PARV, as previously described (Milner et al., 2013; Mazid et al., 2016). Briefly, tissue sections were rinsed in TS and blocked in 0.5% BSA in TS for 30 minutes. Sections were placed in a cocktail of the primary antibodies in 0.1% BSA in TS: DOR (1:5000) + GABA (1:1000) or MOR (1:1000) + PARV (1:3000). Sections were placed on a shaker for 24 hours at room temperature and then for four days at 4°C. Next, sections were processed for peroxidase labeling for GABA (3 minutes in DAB) or PARV (10–12 minutes in DAB reaction) as described above, except that either biotinylated donkey anti-rat IgG (GABA; Jackson Immunoresearch Laboratories, Cat# 712–065-150, RRID:AB_2340646) or horse anti-mouse IgG (PARV; Vector Laboratories Cat# BA-2001; RRID:AB_2336180) was used as a secondary antibody. Sections then were washed in TS and incubated in donkey anti-rabbit IgG (DOR and MOR) conjugated to 1 nm gold particles [diluted 1:50; Electron Microscopy Sciences (EMS) Cat# 810.311, RRID:AB_2629850] in 0.01% gelation and 0.08% BSA dissolved in 0.01 M phosphate-buffered saline (PBS) at 4°C overnight. Tissue sections were rinsed in PBS, postfixed in 2% glutaraldehyde in PBS for 10 minutes, and then rinsed in PBS followed by 0.2 M sodium citrate buffer (pH = 7.4). IgG conjugated gold particles were enhanced by undergoing a reaction for 6–7 minutes with IntenSE-M silver enhancement kit [Amersham Biosciences, Waltham, MA; Cat# RPN491 (discontinued)].

Tissue sections then were fixed in 2% osmium tetroxide for one hour followed by washes in PB and dehydration via increasing concentrations of ethanol and propylene oxide prior to embedding in EMbed 812 (EMS, 14120). Ultrathin sections (approximately 70–72 nm thick) from the hippocampal blocks were cut and collected on 400 mesh thin-bar copper grids (T400-Cu, EMS), which were then counterstained with uranyl acetate (EMS 22400) and Reynolds lead citrate (EMS, 17900–25).

Identification of EM profiles: Tissue sections containing hippocampal ROIs were examined on a CM10 transmission electron microscope (FEI, Hillsboro, OR). Images were captured at a magnification of 13500x and cells were classified as neuronal or glial based on standard morphology (Peters, 1991). Dendrites were identified by their post-synaptic positioning to axons and were classified as large (diameter > 1.0 μm) or small (diameter < 1.0 μm). Irregular or oblong shaped dendrites (form factor < 0.5) were excluded from analysis. Axon terminals were identified by the presence of numerous small synaptic vesicles. Mossy fiber terminals were identified on the basis of the presence of multiple small synaptic vesicles and their large size (approximately 1.5 – 2 μm in diameter) (Pierce et al., 2014). Immunoperoxidase was identified as an electron-dense precipitate with GABA- and PARV-containing dendrites, and silver intensified immunogold (SIG) labeling for DOR and MOR was identified as black electron-dense particles (Milner et al., 2011). Dual labeling was classified as an instance where both electron-dense precipitates and at least one gold particle were observed.

Data were collected and analyzed by investigators who were blind to experimental condition [oxycodone CPP (Oxy) or saline injected (Sal)]. Experimental condition was unblinded after figures were generated.

Analysis 1: dendritic profiles.—For analysis, micrographs containing DOR-SIG or MOR-SIG labeled dendrites were collected from SR of CA3 and the hilus of the DG as described in our previous studies (Mazid et al., 2016; Marques-Lopes et al., 2017). Briefly, 50 randomly selected dual-labeled dendrites were photographed, and the subcellular localization of DOR-SIG or MOR-SIG particles was determined. Microcomputer Imaging Device software (MCID Analysis, RRID:SCR_014278) was used to assess perimeter, cross-sectional area and diameter, and major and minor axis lengths for each dual-labeled dendrite.

Distribution of DOR-SIG or MOR-SIG labeling was analyzed through the following parameters: 1) the number of SIG particles localized to the plasma membrane of the dendrite (PM:μm), 2) the number of SIG particles localized within 50 nm of the plasma membrane (Near PM:μm), 3) the number of SIG particles localized to the cytoplasm per cross-sectional area (CY:μm^2), and 4) the total number of SIG particles per cross-sectional area (Total:μm^2). The partitioning ratio was calculated as the proportion of SIG particles in a given subcellular compartment (i.e., on plasma membrane (PM), near PM, or in the cytoplasm) divided by the total number of DOR-SIG or MOR-SIG particles within the cell.

SIG labeling on the plasma membrane identifies receptor-binding sites whereas SIG labeling near the plasma membrane identifies a pool of receptors from which receptors can be added or removed from the plasma membrane (Boudin et al., 1998). SIG labeling in the cytoplasm identifies receptors that are either stored during transfer to or from the soma or another cellular compartment, or the receptors are being degraded or recycled (Pierce et al., 2009; Fernandez-Monreal et al., 2012). When stimulated by an agonist, the ratio of receptors on the plasma membrane to those in the cytoplasm declines, as demonstrated by the number of SIG labeled receptors in each compartment (Haberstock-Debic et al., 2003).

Analysis 2: DOR-labeled dendritic spines contacted by mossy fibers.—The number of DOR-SIG labeled dendritic spines contacted by mossy fibers in SLu of CA3 was determined using previously described methods (Harte-Hargrove et al., 2015; Mazid et al., 2016). For this, 50 randomly selected mossy fibers contacted by spines from the tissue-plastic interface were photographed. The percentage of labeled spines (i.e., spines containing 1 or more SIG particle) was tallied and then subcellular location of the SIG particle at the synapse, on the plasma membrane or in the cytoplasm was noted.

Analysis 3: DOR-labeled dendritic spines in CA3 SR.—From the SR CA3 micrographs (same micrographs used in Analysis 1), 100 spine profiles per rat were randomly identified. Dendritic spines were included if contacted by a terminal forming an asymmetric synapse and categorized as unlabeled or labeled (with at least one DOR-SIG particle). DOR-SIG particles in labeled dendritic spines were classified as in the synapse, on the plasma membrane, or in the cytoplasm.

Analysis 4: number of MOR/PARV cells in DG.—Using the granule cell layer as a guide, the number of soma dually labeled for MOR and PARV in the dorsal blade of the hilus was determined at 4200x. All dually labeled cells containing a nucleus were counted and divided by the number of squares (each 55 μm in diameter) to determine the number of MOR/PARV cells/mm^2.

Figure Preparation

Image adjustments were applied uniformly to all portions of the image. No specific feature within an image was enhanced, obscured, moved, removed or introduced. Adjustments to sharpness, brightness and contrast were identical between light microscope images from the same experiment and were made in Microsoft Powerpoint 2010. Electron micrographs were increased in resolution (400 dpi) and then adjusted for sharpness (using unsharp mask), brightness, and contrast in Adobe Photoshop 9.0 (Adobe Photoshop, RRID:SCR_014199). Images then were imported into Microsoft Powerpoint 2010 for final layout and labeling. To achieve uniformity in the appearance between micrographs, occasional additional adjustments to brightness and contrast were made in Powerpoint. Graphs were generated using Prism 7 software (Graphpad Prism, RRID:SCR_002798).

Experimental Design and Statistical Analysis

The independent variables in this study were sex (male or female) and drug treatment (saline or oxycodone). Female and male rats (N = 12 per sex) were randomly assigned to either Sal- (control) or Oxy groups (N = 6 per group) for a total of four treatment groups in a 2 × 2 between-subjects design.

Behavior: To assess sex-dependent differences in oxycodone-associated drug learning, rats underwent a 14-day CPP paradigm.

Approach: Immunocytochemistry using antibodies specific for LEnk, DOR, and MOR (described in further detail below) was used to quantify sex or drug treatment-dependent changes in labeling using both light and electron microscopy. To control for variability in

immunoprocessing (Milner et al., 2011), sections were coded with punch tools and cohorts of sections were pooled into single containers and processed simultaneously in all immunocytochemical steps. Two sections per rat [n = 6 per group; 4 groups: Sal-female, Sal-male, Oxy-female, Oxy-male)] were processed for both light and EM studies. For LEnk and DOR light microscopic experiments, one section per rat [n = 6 per group; 4 groups: Sal-female, Sal-male, Oxy-female, Oxy-male)] was analyzed. For the dual label EM experiments, one section from 3 rats per group per region (DOR/GABA: n = 12, SR and SLu of CA3b: n = 12, hilus of DG; MOR/PARV: n = 12, hilus of DG) was cut and analyzed.

Analysis: Data are expressed as mean ± SEM. Significant test statistics were set to an alpha < 0.05. Unless noted, all statistical analyses were conducted on JMP 12 Pro software (JMP, RRID:SCR_014242). CPP data was analyzed using a two-way analysis of variance (ANOVA) followed by a Tukey post-hoc. For this, time spent in the oxycodone-injected box (time spent in oxycodone paired side over the sum of time spent in both the oxycodone- and saline-paired sides) was determined. Locomotor activity was analyzed using a two-way ANOVA (condition x sex) with repeated measures by conditioning session (oxycodone-injection days in sessions 1, 2, 3 and 4) followed by a Bonferroni post-hoc analysis on Prism 7.

Methods for quantitative densitometric analysis of immunoperoxidase reaction product are well established (Auchus and Pickel, 1992; Pierce et al., 2014) and used in numerous studies (Pierce et al., 1999; Williams et al., 2011a; Pierce et al., 2014; Mazid et al., 2016). Light microscopic optical density sample comparisons between Sal-female and Sal-male, Sal-female and Oxy-female or Sal-male and Oxy-male were determined through a two-tailed t-test for samples with equal variances with a Welch correction for samples with unequal variances (as determined by Levene's test) as the data set was underpowered for a two-way ANOVA. The numbers of DOR-labeled or MOR/PARV-labeled cells were analyzed using a Student's t-test comparing Sal-female and Sal-male, Sal-female and Oxy-female or Sal-male and Oxy-male.

Quantitative dual labeling EM methods are designed to determine relative changes in the subcellular distribution of proteins in dendrites of different sizes following experimental manipulations. For this, protein distribution of DORs or MORs in dendritic profiles of different sizes, rather than number of cells or dendrites per animal, is analyzed. Implicit in our analysis are corrections for errors related to spatial location by only analyzing a single plane within a section. In these studies we measure dendritic profile cross-sectional area, perimeter, and average diameter and use these to determine SIG particle density for each dendritic compartment (e.g., PM/μm) to correct for any size-related differences. To analyze redistribution of SIG particles within a dendrite, we divided the number of SIG particles in each compartment by the total number of SIG particles in the dendrite (e.g., PM/total).

Our previous study (Znamensky et al., 2003) randomly sampled dendritic profiles in 9632 μm^2 of tissue and determined that 50 dendritic profiles per block were sufficient to make quantitative comparisons on the subcellular distribution of proteins between groups. In Znamensky et al. (2003), increasing the number of dendrites to 75 or greater per animal did not change the significance of the results. Numerous publications from our laboratory as

well as other laboratories have used this approach for the analysis (Coleman et al., 2013; Marques-Lopes et al., 2014; Glass et al., 2015; Van Kempen et al., 2015; Mazid et al., 2016; McAlinn et al., 2018). Comparisons in DOR-SIG distributions in the Sal-female and Sal-male rats were determined through one-way ANOVA or Welch t-test ANOVAs for samples with unequal variances (as determined by Levene's test). Comparisons were performed for sex, treatment, and the sex by treatment interaction using two-way ANOVAs and Tukey's HSD post-hoc analyses for specific between-group differences.

RESULTS

Females and males acquire oxycodone CPP

Two-way ANOVA showed a significant main effect of condition (oxycodone CPP vs saline) [$F(3,18) = 50.234$, $p < 0.0001$], and sex [$F(3,18) = 4.974$, $p < 0.039$] as well as a significant interaction of sex x condition [$F(3,18) = 6.422$, $p = 0.021$]. Post-hoc revealed that both female ($p < 0.0001$) and male ($p < 0.0224$) rats demonstrated CPP to oxycodone (Fig. 1A) as shown by significant increases in percent time spent in the oxycodone-paired chamber. However, females showed significantly more percent time spent on the oxycodone-paired side than male rats ($p = 0.0222$). On testing day, there were no significant differences in box preference in the saline-injected (Sal) rats.

Two-way repeated measures ANOVA revealed a significant main effect of conditioning session on the locomotion score [$F(1,6) = 14.74$; $p = 0.0086$]. A Bonferroni post-hoc analysis demonstrated a significant decrease in locomotion in oxycodone-injected males ($p = 0.0103$) but not in the oxycodone-injected females ($p = 0.595$) during the first three training sessions (Fig. 1B). However, no significant differences in locomotion were found in either sex in the fourth oxycodone training session. Due to high locomotion scores on pre-test as well as testing days, one oxycodone-injected male and one oxycodone-injected female were excluded from the final behavioral analysis.

On the day of euthanasia, all female rats but two were in the estrus phase of the estrus cycle. One female rat that acquired oxycodone CPP (Oxy-female) was in proestrus and one Oxy-female rat was in diestrus. As our previous studies have shown that estrous cycle phase alters the levels of LEnk-ir in mossy fibers (Torres-Reveron et al., 2008; Pierce et al., 2014) and MOR and DOR densities/distributions in dendrites (Torres-Reveron et al., 2008; Milner et al., 2013; Mazid et al., 2016), the Oxy-female rat in proestrus (the same rat with elevated locomotion) and the Oxy-female rat in diestrus were not used in the anatomical analyses. Thus, all female rats analyzed in the light and electron microscopic studies were in the estrus phase. Additionally, the Oxy-male excluded from the behavioral analysis was not used in the anatomical analysis.

LEnk-levels differ in saline-injected and oxycodone CPP female and male rats

Consistent with our previous studies (Torres-Reveron et al., 2008; Pierce et al., 2014), diffuse LEnk-ir is found in the mossy fiber pathway, contained in the hilus of the DG and in SLu of the CA3a,b,c regions (Fig. 2A). Moreover, also in agreement with these prior studies, Sal-females, all of which were in their elevated estrogen phase, had increased levels of

LEnk-ir within the DG compared to Sal-males: dorsal blade [t(10) = −2.74; p = 0.021], central hilus [t(10) = −2.26; p = 0.047], and crest [t(10) = −2.62; p = 0.026; Fig. 2C]. Oxy-females compared to Sal-females showed a significant decrease in the levels of LEnk-ir in the CA3a [t(9) = 4.51; p = 0.0015; Fig. 2D,E]. Moreover, the LEnk-labeled processes in SLu of CA3a appeared more diffuse in the Oxy-females compared to the Sal-females (Fig. 2E). In contrast, Oxy-males compared to Sal-males showed a significant increase in the levels of LEnk-ir in CA3b [t(9) = −2.52; p = 0.033; Fig. 2B,D].

As previous studies have shown that several types of experimental manipulations can induce the sprouting of mossy fibers into SO of CA3 [reviewed in (Scharfman and MacLusky, 2014)], this region was analyzed in the 4 cohorts. There was no difference in the levels of LEnk-ir in Sal-females and Sal-males or in the Oxy-males and Sal-males in SO (Fig. 2F). However, Oxy-females compared to Sal-females had significantly more LEnk-labeling in SO of CA3 [t(9) = 2.37; p = 0.042; Fig. 2 E,F]. Thus, the levels of LEnk-ir in the mossy fiber pathway decrease in SLu of CA3a in Oxy-females, likely reflecting the sprouting of LEnk-containing mossy fibers to SO, whereas LEnk levels are elevated within mossy fibers in Oxy-males in SLu of CA3b.

The levels of DOR-ir in the CA3 differ in saline-injected females and males

In agreement with our previous work (Commons and Milner, 1997), diffuse DOR-ir was found throughout the layers of CA3 but was most dense in SLu (Fig. 3A). Representative micrographs showing DOR-ir in CA3b from each experimental group are shown in Figure 3B. Sal-females compared to Sal-males showed significantly greater levels of DOR-ir in the SO [t(10) = −2.81; p = 0.0184] and SLu of CA3 [t(10) = −3.86; p = 0.0032; Fig. 3C]. Following oxycodone CPP, there was no significant difference in the levels of DOR-ir in any CA3b lamina in either females or males (Fig. 3C). These results corroborate our previous findings that sex and estrous cycle phase alter DOR-ir in rat pyramidal cell neurons (Williams et al., 2011a; Mazid et al., 2016).

Oxycodone CPP alters the densities of DORs in CA3 dendrites in males

Examples of DOR-SIG labeling in CA3 pyramidal cell dendrites in SR for all four groups are shown in Figure 4A-D. These dendrites had spines, many of which were contacted by terminals forming asymmetric synapses (examples in Fig. 4B,C). Compared to Sal-males, Sal-females had a significantly lower density of DOR-SIG particles on the plasmalemma [F(1,220) = 4.31; p = 0.039], near the plasmalemma [F(1,234) = 21.1; p < 0.0001] and in total [F(1,283) = 9.88; p = 0.0018] in CA3 dendrites (Fig. 5A). Sal-females also showed a lower partitioning ratio of DOR-SIG particles near the plasmalemma [F(1,237) = 20.0; p < 0.0001] and a greater partitioning ratio of DOR-SIG particles in the cytoplasm [F(1,254) = 25.1; p < 0.0001] compared to Sal-males (Fig. 5B).

Two-way ANOVA showed a significant main effect of sex on the density of DOR SIG particles on the plasmalemma [F(1,582) = 5.12; p = 0.024], near the plasmalemma [F(1,582) = 17.4; p < 0.0001], and in total [F(1,582) = 5.38; p = 0.021] in CA3 dendrites. A significant main effect of treatment (saline-injected vs. oxycodone CPP) was found for the density of DOR SIG particles in CA3 dendrites near the plasmalemma [F(1,582) = 6.96; p = 0.0085]

and in the cytoplasm [F(1,582) = 5.95; p = 0.015]. The sex by treatment interaction was significant among near plasmalemmal [F(1,582) = 10.1; p = 0.0015] and total density [F(1,582) = 4.89; p = 0.028] of DOR-SIG particles in CA3 dendrites. When CA3 DOR-labeled dendrites were further divided into large and small dendrites, the ANOVA results were similar (not shown).

Post-hoc analysis revealed significant differences in the density and partitioning ratio of DOR-SIG particles in CA3 dendrites in Oxy-males but not Oxy-females (Fig. 5C-H). Oxy-males compared to the Sal-males demonstrated a decrease in the density (p = 0.0004) and partitioning ratio (p = 0.0004) of DOR SIG particles near the plasmalemma of CA3 dendrites (Fig. 5D,G). Oxy-males compared to Sal-males also showed an increase in the partitioning ratio (p = 0.0008) of cytoplasmic DOR-SIG particles in CA3 dendrites (Fig. 5H).

In summary, these results demonstrate that in the absence oxycodone CPP, males have higher densities of DORs near the plasmalemma of CA3 pyramidal cell dendrites than estrus females. However, following oxycodone CPP, DORs redistribute away from the plasmalemma to the cytoplasm within the CA3 pyramidal cells of males but not females. This suggests that the ability of DOR agonists to bind to CA3 pyramidal cell dendritic shafts may be attenuated in males following oxycodone CPP.

DOR-labeling in CA3 dendritic spines

Consistent with previous studies (Harte-Hargrove et al., 2015; Mazid et al., 2016) DOR-SIG particles were found in dendritic spines contacted by mossy fibers in CA3 SLu (Fig. 6A). The percent of DOR-labeled dendritic spines contacted by mossy fibers (Table 1) was not significantly different between the four groups. Of the labeled spines in CA3 SLu, DOR-SIG particles were primarily found on the plasma membrane or in the cytoplasm for all 4 groups (Table 1). However, the Oxy-males had about twice as much DOR labeling in the cytoplasm of spines than the other 3 groups (Table 1).

In CA3 SR, DOR-SIG particles were observed in dendritic spines in all four groups (examples Fig. 6B,C). Oxy-females compared to Sal-females had more DOR-SIG particles on the plasma membrane and in the cytoplasm of CA3 dendritic spines in SR (Table 1; Fig. 6C). Moreover, only Oxy-female and Oxy-male rats had DOR-SIG labeling located at the synapse of dendritic spines (Table 1; example Fig. 6B).

Together with the findings in dendritic shafts (above), these findings suggest that DORs traffic to CA3 pyramidal cell dendritic spines following oxycodone CPP in both sexes. However, DORs increase in females in SR and in males at the mossy fiber synapses of CA3 suggesting that they are involved in different functional processes within CA3 pyramidal cell neurons.

Following oxycodone CPP, the number of DOR hilar interneurons increases in females

DOR-labeled neurons were primarily found in the hilus of the DG (Fig. 7A). Our previous studies (Commons and Milner, 1996; Williams and Milner, 2011; Mazid et al., 2016) have shown that DOR-ir in these cells colocalizes with GABA as well as somatostatin (SOM),

neuropeptide Y (NPY) and corticotropin releasing factor (CRF) in the rat. The total number of DOR-labeled cells per mm^2 in the hilus was not significantly different in Sal-females and Sal-males (F: 22.83 ± 3.94; M: 21.3 ± 3.57). Moreover, the number of DOR-labeled cells did not differ in the crest (F: 15.8 ± 4.90; M: 11.7 ± 2.11), central hilus (F: 11.7 ± 1.05; M: 17.5 ± 4.23) and dorsal blade (F: 9.44 ± 2.78; M: 10.0 ± 4.47) of Sal-female and Sal-male rats. Analyzed by sex, there were no differences [$t(10) = 1.20$; $p = 0.257$] between saline- and oxycodone-injected rats in total number of hilar DOR cells per mm^2 (FS: 22.8 ± 3.94, FO: 22.6 ± 3.33; MS: 21.3 ± 3.57, MO: 20.6 ± 2.86). However, significantly more [$t(10) = 4.47$, $p = 0.0012$] DOR-labeled cells were observed in the central hilus in Oxy-females (18.3 ± 1.05) compared to Sal-females (11.7 ± 1.05; Fig. 7B). The number of DOR-immunoreactive cells was not different in the Sal- and Oxy-females in the crest (FS: 15.8 ± 4.90; FO: 5.8 ± 2.39) and dorsal blade of the hilus (FS: 9.44 ± 2.78; FO: 11.7 ± 4.61). Additionally, no significant differences were found in the number of DOR-labeled cells in Sal-males compared to Oxy-males in any subregion (dorsal blade - MS: 10.0 ± 4.47; MO: 15.0 ± 3.07; central hilus - MS: 17.5 ± 4.23; MO: 15.8 ± 4.73; crest - MS: 11.7 ± 2.11; MO: 20.8 ± 3.96). These findings indicate that oxycodone CPP induces an upregulation of DORs selectively in central hilar neurons in females. Moreover, as our EM analysis focused on the crest and central hilus, it is likely that DOR-labeling was detected in more dendrites in the Oxy-females compared to the other three groups.

Oxycodone CPP differentially alters DOR density and redistribution in females and males

Examples of DOR-SIG labeling in GABA-labeled hilar dendrites are shown for all four groups in Figure 8A-D. In both females and males, numerous terminals forming asymmetric synapses contacted the dual-labeled dendrites (examples in Fig. 8A,B). Compared to Sal-males, Sal-females had a greater density [$F(1,269) = 4.76$; $p = 0.03$] and higher partitioning ratio [$F(1,269) = 4.27$; $p = 0.04$] of DOR-SIG particles on the plasma membrane of GABA-labeled dendrites (Fig. 9A,B). This finding is consistent with our previous study (Mazid et al. (2016).

Two-way ANOVA showed a significant main effect of treatment (saline-injection vs. oxycodone CPP) in DOR-SIG density near the membrane of GABA-labeled dendrites [$F(1,604) = 10.8$; $p = 0.0011$]. Main effects of treatment also were seen in near plasmalemmal [$F(1,640) = 9.87$; $p = 0.0018$] and cytoplasmic [$F(1,640) = 4.51$; $p = 0.034$] DOR-SIG partitioning ratios in GABA dendrites. Sex by treatment interaction was significant for the density of DOR-SIGs in GABA dendrites in the cytoplasm [$F(1,640) = 5.54$; $p = 0.019$] and in total [$F(1,640) = 4.25$; $p = 0.040$], as well as partitioning ratio on the plasmalemma [$F(1,640) = 4.37$; $p = 0.037$].

Post-hoc analysis revealed significant differences in the density and partitioning ratio of DORs in GABA-labeled dendrites in both females and males (Fig. 9C-H). Oxy-females compared to Sal-females demonstrated a significant increase in DOR-SIG density ($p = 0.0096$) and partitioning ratio ($p = 0.0032$) near the plasmalemma of GABA-labeled dendrites (Fig. 9D,H). In contrast, Oxy-males compared to Sal-males showed a significant decrease ($p = 0.051$) in the density of DOR-SIG particles in the cytoplasm of GABA-labeled dendrites (Fig. 9E). Sal- and Oxy-males showed no differences in the partitioning ratio of

DOR-SIG particles in any cellular compartment of GABA-labeled dendrites (Fig. 9G,H). Together, these results suggest that in Sal-females DORs in GABAergic interneuron dendrites are positioned to be more sensitive to DOR agonists, and that this is further enhanced following oxycodone CPP. In contrast, oxycodone CPP has little effect on the distribution of DORs in GABAergic dendrites in males.

Oxycodone CPP redistributes MORs in PARV dendrites in females but not males

The crest and central hilar regions of the DG were sampled for electron microscopy. PARV-labeled cells are primarily found in the subgranular zone (Fig. 10A). Consistent with our previous studies (Torres-Reveron et al., 2009a; Milner et al., 2013), MOR-SIG labeling was colocalized with PARV in soma and dendrites (Fig.10B-F). There were no differences in the number of cells per mm^2 dually labeled for MOR and PARV in the dorsal blade of the hilus (Fig. 10B; FS: 10.8 ± 3.1; FO: 7.9 ± 0.4; MS: 9.0 ± 1.2; MO: 6.6 ± 1.6; N =3 rats/condition). Representative micrographs of dendrites dually labeled for MOR-SIG and PARV-immunoperoxidase from each experimental group are presented in Figure 10C-F. In both females and males, numerous terminals formed asymmetric synapses on the MOR/PARV labeled dendrites. Dual labeled axons and terminals (not shown) also were observed in all four groups.

Sal-females showed a lower density of MOR-SIG particles in PARV-labeled dendrites on the plasmalemma [$F(1,190) = 14.1$; $p = 0.0002$], near the plasmalemma [$F(1,212) = 4.16$; $p = 0.043$], within the cytoplasm [$F(1,259) = 10.1$; $p = 0.0017$] and in total [$F(1,267) = 13.73$; $p = 0.0003$; Fig 11A] compared to Sal-males. However, Sal-females showed a greater proportion of MOR-SIG particles near the plasma membrane (i.e., partitioning ratio) of PARV-labeled dendrites compared to Sal-males [$F(1,265) = 4.32$; $p = 0.039$; Fig. 11B].

Two-way ANOVA revealed significant main effects of treatment (i.e., saline-injected vs oxycodone CPP) in total MOR-SIG density in PARV dendrites [$F(1,525) = 3.95$; $p = 0.047$] and a main effect of sex on cytoplasmic MOR-SIG density in PARV dendrites [$F(1,525) = 4.89$; $p = 0.028$]. Sex by treatment interactions were significant for MOR-SIG densities in PARV dendrites on the plasmalemma [$F(1,525) = 11.1$; $p = 0.0009$], in the cytoplasm [$F(1,525) = 5.07$; $p = 0.025$], and in total [$F(1,525) = 13.5$; $p = 0.0003$]. Sex by treatment interactions also were significant for the near plasmalemmal partitioning ratio of MOR-SIG densities in PARV dendrites [$F(1,525) = 5.61$, $p = 0.0183$]. When MOR/PARV-labeled dendrites were separated into large (i.e., proximal) and small (i.e., distal), ANOVA results were similar (not shown).

Post-hoc analyses demonstrated that Oxy-females compared to Sal-females had a significant increase in MOR-SIG density on the plasmalemma ($p = 0.0027$) and in total ($p = 0.0005$) in PARV-labeled dendrites (Fig. 11C,F). Sal- and Oxy-males demonstrated no significant differences in the density of MOR-SIG particles in PARV dendrites (Fig. 11C-F). Although a significant sex by treatment main effect was seen, there were no significant differences in partitioning ratio following oxycodone CPP in females or males in any cellular component (Fig. 11G,H).

Together, these results show that the densities of MORs in PARV interneuron dendrites are elevated in all cellular compartments in Sal-males compared to Sal-females. However, in saline rats, the pool of MORs that can be readily inserted into the plasma membrane of these dendrites is greater in females. Moreover, oxycodone CPP induces processes that allow for dendrites of PARV-containing hilar interneurons in females to more readily bind MOR agonists, e.g., oxycodone.

DISCUSSION

This study shows that both female and male Sprague-Dawley rats acquire oxycodone CPP. However, oxycodone CPP results in sex-dependent changes in the hippocampal opioid system in a manner that would promote excitation and opiate-associative learning processes to a greater degree in females (Fig. 12).

Sex differences in Oxycodone CPP

Like mice (Collins et al., 2016), female and male rats acquired oxycodone CPP and had no differences in locomotion scores in the saline- or oxycodone-sides on the last day of testing. However, in contrast to mice (Niikura et al., 2013; Collins et al., 2016) female and male rats had a pre-test side preference for the CPP chamber and Oxy-males had decreased locomotion in the first three conditioning sessions. Our studies are consistent with studies showing that although morphine initially suppresses locomotor activity in both female and male rats, males are more sensitive to these effects (Craft et al., 2006). Underlying sex differences in mesolimbic dopaminergic function (Almey et al., 2016) have been suggested to contribute to opioid locomotor-activating effects (Craft et al., 2006).

Sex differences in oxycodone CPP agree with results using morphine. Although morphine CPP is achieved in female and male rats at high doses (7.5 mg/kg), female rats acquire CPP with a lower dose of morphine (0.5 mg/kg) and have more pronounced responses with higher doses of morphine (5–10 mg/kg) (Karami and Zarrindast, 2008). However, there are significant differences between oxycodone and morphine in terms of their pharmacodynamics and effects on opioid signaling. While both oxycodone and morphine are MOR agonists, oxycodone exhibits lower efficacy for the MOR receptor under certain conditions (Lemberg et al., 2006). Oxycodone and morphine display distinct post receptor-binding effects on drug internalization and receptor densitization (Bolan et al., 2002; He et al., 2002; Arttamangkul et al., 2008). Additionally, oxycodone is a partial agonist for kappa opioid receptors (KOR), although the extent to which oxycodone activates KORs is limited (Nielsen et al., 2007; Narita et al., 2008). In humans, oxycodone displays a higher and more stable bioavailability compared to morphine (Soderberg Lofdal et al., 2013), an effect which is likely linked to it's greater potency (2 – 4x) than morphine in rats (Poyhia and Kalso, 1992). Nevertheless, the fact that females consistently show a pronounced preference and sensitivity to MOR agonists compared to males suggests that these drugs exert a conserved, sex-dependent action on opioid signaling in the context of drug addiction.

After Oxycodone CPP, LEnk-containing mossy fibers could promote enhanced CA3 pyramidal cell plasticity in both sexes

LEnk-containing mossy fibers are differentially altered in male and female rats following oxycodone CPP in a fashion that would promote synaptic plasticity. Within mossy fibers, LEnk is stored in dense-core vesicles (Pierce et al., 1999; Pierce et al., 2014) and is preferentially released at low frequencies (2 Hz) rather than high frequencies (> 50 Hz) (Wong and Moss, 1992; Han, 2003; Liang et al., 2010). Our previous studies have shown that the elevated LEnk levels in mossy fibers together with the increased DORs in mossy fiber-spine synapses in proestrus (high estrogen) rats are important for the induction of low-frequency opioid dependent LTP in CA3b pyramidal neurons (Harte-Hargrove et al., 2015). In males, the observed elevation of mossy fiber LEnk levels in CA3b following oxycodone CPP suggests that greater amounts of LEnk could be released in response to a low-frequency stimulus.

Following oxycodone CPP, LEnk levels in mossy fibers remained elevated in CA3b and the hilus of estrus females suggesting that the potential for high levels of LEnk release are still in place. Moreover, concurrent with a decrease in LEnk levels in CA3a, where the endings of the mossy fiber projection reside (Torres-Reveron et al., 2008), LEnk-containing mossy fibers sprouted into the SO of CA3 in the females following oxycodone CPP. Mossy fiber sprouting has been shown to be associated with increased synaptic plasticity (Scharfman and MacLusky, 2014).

In addition to opioid peptides, mossy fibers contain phosphorylated MORs at similar levels in both females and males (Gonzales et al., 2011). Earlier studies have shown that the MORs in the mossy fibers are the MOR1D splice variant, in which exon 4 is replaced by exon 8 and 9 (Abbadie et al., 2000). As opioid agonists have a high binding affinity for MOR1D (Bolan et al., 2004), oxycodone then could directly affect LEnk release within mossy fibers.

After oxycodone CPP, DORs redistribute within CA3 pyramidal cells in both sexes in a manner that could promote excitation

Following oxycodone CPP, DORs redistribute in different portions of the CA3b pyramidal cell dendrites in the two sexes. In Oxy-males compared to Sal-males, near-plasmalemma DORs trafficked to the cytoplasm of SR dendrites; moreover, the number of DORs in mossy fiber-spine synapses increased. Although this rearrangement of DORs would make the CA3b pyramidal cells less sensitive to opioid agonists, the increase in DORs at the mossy fiber-spine synapses together with the observed increase in LEnks, which have a high affinity for DORs (Corbett et al., 1993), suggest that the likelihood for excitation and opioid-dependent LTP at the mossy fiber-CA3 synapse (Moore et al., 1994; Harte-Hargrove et al., 2015) is increased in males.

In Sal- and Oxy-females, the distribution of DORs in mossy fiber-spine synapses and the levels of LEnk in mossy fibers is similar, suggesting that the potential for low frequency opioid-dependent LTP (Harte-Hargrove et al., 2015) is still in place. However, our observation that DORs are more prevalent on the dendritic spines of distal SR CA3b

pyramidal cell dendrites in Oxy-females suggests that opioid agonists could exert a greater effect on CA3 afferent signaling following oxycodone CPP.

We previously showed (Burstein et al., 2013) that morphine elevates phosphorylated DORs, which are important for uncoupling and internalization of DORs (Pradhan et al., 2009), on CA2/3 pyramidal neurons. DORs are associated with beta-arrestin, which is involved in the trafficking of G-protein coupled receptors and signal transduction (Cen et al., 2001; Shenoy and Lefkowitz, 2011). In particular, DORs can modulate CRF receptor 1 (CRFR1) signaling (Markovic et al., 2006; Williams et al., 2011b; Dunn et al., 2013). Males have greater numbers of CRFR1s on the plasmalemma of CA3 pyramidal cell neurons (McAlinn et al., 2018). The interaction of DORs with CRFR1 in hippocampal neurons could contribute to sex differences in the response of these neurons, as well as hilar interneurons following acute and chronic stress (Mazid et al., 2016).

Following oxycodone CPP, DORs and MORs are positioned in interneurons to promote more disinhibition in females

In Sal-females compared to Sal-males, plasmalemmal DORs are greater on the dendrites of GABA-labeled interneurons that previous studies have shown colocalize SOM and NPY (Commons and Milner, 1996; Williams and Milner, 2011; Mazid et al., 2016). Conversely, Sal-females compared to Sal-males have fewer plasmalemmal MORs on the dendrites of PARV-containing interneurons. In Oxy-females only, the number of DOR-labeled hilar interneurons increased and the pool of near-plasmalemmal DORs in GABA-labeled dendrites as well as plasmalemmal and total MORs in PARV-labeled dendrites increased. Thus, initially DORs and MORs in the DG hilus are positioned to promote disinhibition of different populations of interneurons. Following oxycodone CPP, the possibility for disinhibition of both DOR- and MOR-containing interneurons is enhanced in females.

This redistribution of DORs and MORs in hilar interneurons could affect the manner in which the cells integrate into the functional circuit. Hilar SOM/NPY interneurons project to granule cell dendrites where they converge with entorhinal afferents (Milner and Bacon, 1989; Milner and Veznedaroglu, 1992). Since DORs inhibit NPY release, activation of DORs on NPY-containing GABA interneurons could promote lateral perforant pathway LTP (Sperk et al., 2007). Interestingly, chronic immobilization stress (CIS) results in a similar rearrangement of DORs and MORs in hilar interneurons in females and males as the present study observed after oxycodone CPP (Mazid et al., 2016). Females are more susceptible to several aspects of addiction than males including escalation to drug use and relapse due to stressful events (Becker et al., 2017). Whether CIS could have a sex-specific effect on oxycodone CPP is an area of future investigation by our laboratories.

Functional implications

Overall, the present findings indicate that opioid peptides, MORs and DORs redistribute differently in hippocampal circuits of males and females following oxycodone CPP. In particular, after oxycodone CPP DORs redistributed in mossy fiber-CA3 synapses in males in a manner that resembles what happens in females, which we previously showed is important for opioid-mediated LTP (Harte-Hargrove et al., 2015). However, after oxycodone

CPP MORs and DORs redistributed in hilar interneurons in females in a manner that would enhance disinhibition of granule cells via two different circuits and thus facilitate plasticity processes important in opioid-associated learning processes. This may help explain a greater susceptibility of females to opioid addiction acquisition and relapse (Becker et al., 2017).

These findings add to a growing body of literature that has increasingly emphasized the importance of sex differences in the response to drugs of abuse, particularly to opioids including oxycodone. More prospective studies and rigorous clinical research is needed to determine if the sex-specific effects of oxycodone seen in rats occur in humans.

Acknowledgements

Supported by NIH grants DA08259 (T.A.M., M.J.K., B.S.M.), HL098351 (T.A.M.), HL 136520 (T.A.M.), MH041256 (B.S.M.) and MH102065 (J.D.G.), and Hope for Depression Research grant (B.S.M.). We thank Ms. Batsheva Reich for assistance with figure preparation and Dr. Diane Lane for help with statistical analysis of behavioral data.

ABBREVIATIONS

ABC	avidin-biotin complex
ANOVA	analysis of variance
BSA	bovine serum albumin
cen	central hilus
CIS	chronic immobilization stress
CPP	conditioned place preference
cr	crest of hilus
CRF	corticotropin releasing factor
CRFR1	corticotropin releasing factor receptor 1
DAB	diaminobenzidine
db	dorsal blade of hilus
DG	dentate gyrus
DOR	delta opioid receptor
gc	granule cell
gcl	granule cell layer
EM	electron microscopic
KOR	kappa opioid receptor
LEnk	Leucine-enkephalin

lpp	lateral perforant path
LTP	long-term potentiation
mf	mossy fiber
ML	molecular layer
MOR	mu opioid receptor
N	nucleus
NPY	neuropeptide Y
Oxy	oxycodone CPP rat
PARV	parvalbumin
PFA	paraformaldehyde
PB	phosphate buffer
PBS	phosphate-buffered saline
ROI	region of interest
Sal	saline CPP rat
SIG	silver-intensified immunogold
SLu	Stratum lucidum
SO	Stratum oriens
SR	Stratum radiatum
SOM	somatostatin
TS	tris-buffered saline

References

Abbadie C, Pan Y, Drake CT, Pasternak GW (2000) Comparative immunohistochemical distributions of carboxy terminus epitopes from the mu-opioid receptor splice variants mor-1d, mor-1 and mor-1c in the mouse and rat cns. Neuroscience 100:141–153. [PubMed: 10996465]

Almey A, Milner TA, Brake WG (2016) Estrogen receptor alpha and g-protein coupled estrogen receptor 1 are localized to GABAergic neurons in the dorsal striatum. Neurosci Lett 622:118–123. [PubMed: 27080432]

Arttamangkul S, Quillinan N, Low MJ, von Zastrow M, Pintar J, Williams JT (2008) Differential activation and trafficking of mu-opioid receptors in brain slices. Mol Pharmacol 74:972–979. [PubMed: 18612077]

Arvidsson U, Riedl M, Chakrabarti S, Lee JH, Nakano AH, Dado RJ, Loh HH, Law PY, Wessendorf MW, Elde R (1995) Distribution and targeting of a mu-opioid receptor (MOR1) in brain and spinal cord. J Neurosci 15:3328–3341. [PubMed: 7751913]

Auchus AP, Pickel VM (1992) Quantitative light microscopic demonstration of increased pallidal and striatal met^5-enkephalin-like immunoreactivity in rats following chronic treatment with haloperidol

but not with clozapine: Implications for the pathogenesis of neuroleptic-induced movement disorders. Exp Neurol 117:17–27. [PubMed: 1618284]

Barg J, Levy R, Simantov R (1984) Up-regulation of opiate receptors by opiate antagonists in neuroblastoma-glioma cell culture: The possibility of interaction with guanosine triphosphate-binding proteins. Neurosci Lett 50:133–137. [PubMed: 6093009]

Becker JB, McClellan ML, Reed BG (2017) Sex differences, gender and addiction. J Neurosci Res 95:136–147. [PubMed: 27870394]

Berke JD, Hyman SE (2000) Addiction, dopamine, and the molecular mechanisms of memory. Neuron 25:515–532. [PubMed: 10774721]

Bie B, Zhang Z, Cai YQ, Zhu W, Zhang Y, Dai J, Lowenstein CJ, Weinman EJ, Pan ZZ (2010) Nerve growth factor-regulated emergence of functional delta-opioid receptors. J Neurosci 30:5617–5628. [PubMed: 20410114]

Bolan EA, Tallarida RJ, Pasternak GW (2002) Synergy between mu opioid ligands: Evidence for functional interactions among mu opioid receptor subtypes. J Pharmacol Exp Ther 303:557–562. [PubMed: 12388636]

Bolan EA, Pan YX, Pasternak GW (2004) Functional analysis of mor-1 splice variants of the mouse mu opioid receptor gene OPRm. Synapse 51:11–18. [PubMed: 14579421]

Boudin H, Pelaprat D, Rostene W, Pickel VM, Beaudet A (1998) Correlative ultrastructural distribution of neurotensin receptor proteins and binding sites in the rat substantia nigra. J Neurosci 18:8473–8484. [PubMed: 9763490]

Burstein SR, Williams TJ, Lane DA, Knudsen MG, Pickel VM, McEwen BS, Waters EM, Milner TA (2013) The influences of reproductive status and acute stress on the levels of phosphorylated delta opioid receptor immunoreactivity in rat hippocampus. Brain Res 1518:71–81. [PubMed: 23583481]

Celio MR (1990) Calbindin D-28k and parvalbumin in the rat nervous system. Neuroscience 35:375–475. [PubMed: 2199841]

Celio MR, Baier W, Scharer L, de Viragh PA, Gerday C (1988) Monoclonal antibodies directed against the calcium binding protein parvalbumin. Cell Calcium 9:81–86. [PubMed: 3383226]

Cen B, Yu Q, Guo J, Wu Y, Ling K, Cheng Z, Ma L, Pei G (2001) Direct binding of beta-arrestins to two distinct intracellular domains of the delta opioid receptor. J Neurochem 76:1887–1894. [PubMed: 11259507]

Coleman CG, Wang G, Faraco G, Marques Lopes J, Waters EM, Milner TA, Iadecola C, Pickel VM (2013) Membrane trafficking of NADPH oxidase p47(phox) in paraventricular hypothalamic neurons parallels local free radical production in angiotensin II slow-pressor hypertension. J Neurosci 33:4308–4316. [PubMed: 23467347]

Collins D, Reed B, Zhang Y, Kreek MJ (2016) Sex differences in responsiveness to the prescription opioid oxycodone in mice. Pharmacol Biochem Behav 148:99–105. [PubMed: 27316549]

Commons KG, Milner TA (1995) Ultrastructural heterogeneity of enkephalin-containing terminals in the rat hippocampal formation. J Comp Neurol 358:324–342. [PubMed: 7560290]

Commons KG, Milner TA (1996) Cellular and subcellular localization of delta opioid receptor immunoreactivity in the rat dentate gyrus. Brain Res 738:181–195. [PubMed: 8955512]

Commons KG, Milner TA (1997) Localization of delta opioid receptor immunoreactivity in interneurons and pyramidal cells in the rat hippocampus. J Comp Neurol 381:373–387. [PubMed: 9133574]

Corbett AD, Paterson SJ, Kosterlitz HW (1993) Selectivity of ligands for opioid receptors. In: Opioids (Herz A, Akil H, Simon EJ, eds), pp 645–679. Berlin, Heidelberg: Springer Berlin Heidelberg.

Craft RM, Clark JL, Hart SP, Pinckney MK (2006) Sex differences in locomotor effects of morphine in the rat. Pharmacol Biochem Behav 85:850–858. [PubMed: 17217999]

Crain BJ, Chang KJ, McNamara JO (1986) Quantitative autoradiographic analysis of mu and delta opioid binding sites in the rat hippocampal formation. J Comp Neurol 246:170–180. [PubMed: 3007584]

Deutsch-Feldman M, Picetti R, Seip-Cammack K, Zhou Y, Kreek MJ (2015) Effects of handling and vehicle injections on adrenocorticotropic and corticosterone concentrations in sprague-dawley compared with lewis rats. J Am Assoc Lab Anim Sci 54:35–39. [PubMed: 25651089]

Drake CT, Milner TA (1999) Mu opioid receptors are in somatodendritic and axonal compartments of gabaergic neurons in rat hippocampal formation. Brain Res 849:203–215. [PubMed: 10592303]

Drake CT, Milner TA (2006) Mu opioid receptors are extensively co-localized with parvalbumin, but not somatostatin, in the dentate gyrus. Neurosci Lett 403:176–180. [PubMed: 16716508]

Drake CT, Chavkin C, Milner TA (2007) Opioid systems in the dentate gyrus. Prog Brain Res 163:245–263. [PubMed: 17765723]

Centers for disease control and prevention (2015). Drug overdose deaths hit record numbers in 2014 (Retrieved from) https://www.cdc.gov/media/releases/2015/p1218-drug-overdose.html.

Dunn HA, Walther C, Godin CM, Hall RA, Ferguson SSG (2013) Role of sap97 protein in the regulation of corticotropin-releasing factor receptor 1 endocytosis and extracellular signal-regulated kinase 1/2 signaling. J Biol Chem 288:15023–15034. [PubMed: 23576434]

Fernandez-Monreal M, Brown TC, Royo M, Esteban JA (2012) The balance between receptor recycling and trafficking toward lysosomes determines synaptic strength during long-term depression. J Neurosci 32:13200–13205. [PubMed: 22993436]

Gillies GE, Virdee K, McArthur S, Dalley JW (2014) Sex-dependent diversity in ventral tegmental dopaminergic neurons and developmental programing: A molecular, cellular and behavioral analysis. Neuroscience 282:69–85. [PubMed: 24943715]

Glass MJ, Wang G, Coleman CG, Chan J, Ogorodnik E, Van Kempen TA, Milner TA, Butler SD, Young CN, Davisson RL, Iadecola C, Pickel VM (2015) NMDA receptor plasticity in the hypothalamic paraventricular nucleus contributes to the elevated blood pressure produced by angiotensin II. J Neurosci 35:9558–9567. [PubMed: 26134639]

Gonzales KL, Chapleau JD, Pierce JP, Kelter DT, Williams TJ, Torres-Reveron A, McEwen BS, Waters EM, Milner TA (2011) The influences of reproductive status and acute stress on the levels of phosphorylated mu opioid receptor immunoreactivity in rat hippocampus. Front Endocrinol 2: 1–10.

Gulya K, Gehlert DR, Wamsley JK, Mosberg H, Hruby VJ, Yamamura HI (1986) Light microscopic autoradiographic localization of delta opioid receptors in the rat brain using a highly selective bis-penicillamine cyclic enkephalin analog. J Pharmacol Exp Ther 238:720–726. [PubMed: 3016247]

Haberstock-Debic H, Wein M, Barrot M, Colago EE, Rahman Z, Neve RL, Pickel VM, Nestler EJ, von Zastrow M, Svingos AL (2003) Morphine acutely regulates opioid receptor trafficking selectively in dendrites of nucleus accumbens neurons. J Neurosci 23:4324–4332. [PubMed: 12764121]

Han JS (2003) Acupuncture: Neuropeptide release produced by electrical stimulation of different frequencies. Trends Neurosci 26:17–22. [PubMed: 12495858]

Harte-Hargrove LC, Varga-Wesson A, Duffy AM, Milner TA, Scharfman HE (2015) Opioid receptor-dependent sex differences in synaptic plasticity in the hippocampal mossy fiber pathway of the adult rat. J Neurosci 35:1723–1738. [PubMed: 25632146]

He L, Fong J, von Zastrow M, Whistler JL (2002) Regulation of opioid receptor trafficking and morphine tolerance by receptor oligomerization. Cell 108:271–282. [PubMed: 11832216]

Hyman SE, Malenka RC, Nestler EJ (2006) Neural mechanisms of addiction: The role of reward-related learning and memory. Annu Rev Neurosci 29:565–598. [PubMed: 16776597]

Karami M, Zarrindast MR (2008) Morphine sex-dependently induced place conditioning in adult wistar rats. Eur J Pharmacol 582:78–87. [PubMed: 18191832]

Kesner RP, Warthen DK (2010) Implications of CA3 nmda and opiate receptors for spatial pattern completion in rats. Hippocampus 20:550–557. [PubMed: 19650123]

Kieffer BL, Befort K, Gaveriaux-Ruff C, Hirth CG (1992) The delta-opioid receptor: Isolation of a cDNA by expression cloning and pharmacological characterization. Proc Natl Acad Sci U S A 89:12048–12052. [PubMed: 1334555]

Koob GF, Volkow ND (2010) Neurocircuitry of addiction. Neuropsychopharmacology 35:217–238. [PubMed: 19710631]

Lacy RT, Strickland JC, Feinstein MA, Robinson AM, Smith MA (2016) The effects of sex, estrous cycle, and social contact on cocaine and heroin self-administration in rats. Psychopharmacology (Berl) 233:3201–3210. [PubMed: 27370020]

Lauder JM, Han VK, Henderson P, Verdoorn T, Towle AC (1986) Prenatal ontogeny of the GABAergic system in the rat brain: An immunocytochemical study. Neuroscience 19:465–493. [PubMed: 3022187]

Lemberg KK, Kontinen VK, Siiskonen AO, Viljakka KM, Yli-Kauhaluoma JT, Korpi ER, Kalso EA (2006) Antinociception by spinal and systemic oxycodone: Why does the route make a difference? In vitro and in vivo studies in rats. Anesthesiology 105:801–812. [PubMed: 17006080]

Liang J, Ping XJ, Li YJ, Ma YY, Wu LZ, Han JS, Cui CL (2010) Morphine-induced conditioned place preference in rats is inhibited by electroacupuncture at 2 hz: Role of enkephalin in the nucleus accumbens. Neuropharmacology 58:233–240. [PubMed: 19596017]

Mansour A, Khachaturian H, Lewis ME, Akil H, Watson SJ (1987) Autoradiographic differentiation of mu, delta, and kappa opioid receptors in the rat forebrain and midbrain. J Neurosci 7:2445–2464. [PubMed: 3039080]

Mansour A, Fox CA, Burke S, Meng F, Thompson RC, Akil H, Watson SJ (1994) Mu, delta, and kappa opioid receptor mrna expression in the rat cns: An *in situ* hybridization study. J Comp Neurol 350:412–438. [PubMed: 7884049]

Markovic D, Papadopoulou N, Teli T, Randeva H, Levine MA, Hillhouse EW, Grammatopoulos DK (2006) Differential responses of corticotropin-releasing hormone receptor type 1 variants to protein kinase C phosphorylation. Journal of Pharmacology and Experimental Therapeutics 319:1032–1042. [PubMed: 16956982]

Marques-Lopes J, Van Kempen T, Waters EM, Pickel VM, Iadecola C, Milner TA (2014) Slow-pressor angiotensin II hypertension and concomitant dendritic nmda receptor trafficking in estrogen receptor beta-containing neurons of the mouse hypothalamic paraventricular nucleus are sex and age dependent. J Comp Neurol 522:3075–3090. [PubMed: 24639345]

Marques-Lopes J, Tesfaye E, Israilov S, Van Kempen TA, Wang G, Glass MJ, Pickel VM, Iadecola C, Waters EM, Milner TA (2017) Redistribution of NMDA receptors in estrogen-receptor-beta-containing paraventricular hypothalamic neurons following slow-pressor angiotensin II hypertension in female mice with accelerated ovarian failure. Neuroendocrinology 104:239–256. [PubMed: 27078860]

Mavrikaki M, Pravetoni M, Page S, Potter D, Chartoff E (2017) Oxycodone self-administration in male and female rats. Psychopharmacology (Berl) 234:977–987. [PubMed: 28127624]

Mazid S, Hall BS, Odell SC, Stafford K, Dyer AD, Van Kempen TA, Selegean J, McEwen BS, Waters EM, Milner TA (2016) Sex differences in subcellular distribution of delta opioid receptors in the rat hippocampus in response to acute and chronic stress. Neurobiol Stress 5:37–53. [PubMed: 27981195]

McAlinn HR, Reich B, Contoreggi NH, Kamakura RP, Dyer AG, McEwen BS, Waters EM, Milner TA (2018) Sex differences in the subcellular distribution of corticotropin-releasing factor receptor 1 in the rat hippocampus following chronic immobilization stress. Neuroscience 383:98–113. [PubMed: 29753863]

McEwen BS, Milner TA (2017) Understanding the broad influence of sex hormones and sex differences in the brain. J Neurosci Res 95:24–39. [PubMed: 27870427]

McLean S, Rothman RB, Jacobson AE, Rice KC, Herkenham M (1987) Distribution of opiate receptor subtypes and enkephalin and dynorphin immunoreactivity in the hippocampus of squirrel, guinea pig, rat, and hamster. J Comp Neurol 255:497–510. [PubMed: 2880880]

Meilandt WJ, Barea-Rodriguez E, Harvey SA, Martinez JL, Jr., (2004) Role of hippocampal CA3 mu-opioid receptors in spatial learning and memory. J Neurosci 24:2953–2962. [PubMed: 15044534]

Milner TA, Bacon CE (1989) Ultrastructural localization of somatostatin-like immunoreactivity in the rat dentate gyrus. J Comp Neurol 290:544–560. [PubMed: 2613944]

Milner TA, Veznedaroglu E (1992) Ultrastructural localization of neuropeptide Y-like immunoreactivity in the rat hippocampal formation. Hippocampus 2:107–125. [PubMed: 1308177]

Milner TA, Pickel VM, Reis DJ (1989) Ultrastructural basis for interactions between central opioids and catecholamines. I. Rostral ventrolateral medulla. J Neurosci 9:2114–2130. [PubMed: 2566665]

Milner TA, Burstein SR, Marrone GF, Khalid S, Gonzalez AD, Williams TJ, Schierberl KC, Torres-Reveron A, Gonzales KL, McEwen BS, Waters EM (2013) Stress differentially alters mu opioid receptor density and trafficking in parvalbumin-containing interneurons in the female and male rat hippocampus. Synapse 67:757–772. [PubMed: 23720407]

Milner TA, Waters EM, Robinson DC, Pierce JP (2011) Degenerating processes identified by electron microscopic immunocytochemical methods. Neurodegeneration, Methods and Protocols:23–59.

Moore SD, Madamba SG, Schweitzer P, Siggins GR (1994) Voltage-dependent effects of opioid peptides on hippocampal CA3 pyramidal neurons in vitro. J Neurosci 14:809–820. [PubMed: 7905518]

Narita M, Nakamura A, Ozaki M, Imai S, Miyoshi K, Suzuki M, Suzuki T (2008) Comparative pharmacological profiles of morphine and oxycodone under a neuropathic pain-like state in mice: Evidence for less sensitivity to morphine. Neuropsychopharmacology 33:1097–1112. [PubMed: 17593930]

Nielsen CK, Ross FB, Lotfipour S, Saini KS, Edwards SR, Smith MT (2007) Oxycodone and morphine have distinctly different pharmacological profiles: Radioligand binding and behavioural studies in two rat models of neuropathic pain. Pain 132:289–300. [PubMed: 17467904]

Niikura K, Ho A, Kreek MJ, Zhang Y (2013) Oxycodone-induced conditioned place preference and sensitization of locomotor activity in adolescent and adult mice. Pharmacol Biochem Behav 110:112–116. [PubMed: 23827650]

Olive MF, Anton B, Micevych P, Evans CJ, Maidment NT (1997) Presynaptic versus postsynaptic localization of mu and delta opioid receptors in dorsal and ventral striatopallidal pathways. J Neurosci 17:7471–7479. [PubMed: 9295393]

Olmstead MC, Burns LH (2005) Ultra-low-dose naltrexone suppresses rewarding effects of opiates and aversive effects of opiate withdrawal in rats. Psychopharmacology (Berl) 181:576–581. [PubMed: 16010543]

Ordonez Gallego A, Gonzalez Baron M, Espinosa Arranz E (2007) Oxycodone: A pharmacological and clinical review. Clin Transl Oncol 9:298–307. [PubMed: 17525040]

Persson AI, Thorlin T, Eriksson PS (2005) Comparison of immunoblotted delta opioid receptor proteins expressed in the adult rat brain and their regulation by growth hormone. Neurosci Res 52:1–9. [PubMed: 15811547]

Peters A, Palay SL, Webster H.d. (1991) The fine structure of the nervous system: Neurons and their supporting cells, 3 Edition. New York: Oxford University Press.

Pierce JP, Kurucz OS, Milner TA (1999) Morphometry of a peptidergic transmitter system: Dynorphin B-like immunoreactivity in the rat hippocampal mossy fiber pathway before and after seizures. Hippocampus 9:255–276. [PubMed: 10401641]

Pierce JP, Kelter DT, McEwen BS, Waters EM, Milner TA (2014) Hippocampal mossy fiber leu-enkephalin immunoreactivity in female rats is significantly altered following both acute and chronic stress. J Chem Neuroanat 55:9–17. [PubMed: 24275289]

Pierce JP, Kievits J, Graustein B, Speth RC, Iadecola C, Milner TA (2009) Sex differences in the subcellular distribution of AT(1) receptors and nadph oxidase subunits in the dendrites of C1 neurons in the rat rostral ventrolateral medulla. Neuroscience 163:329–338. [PubMed: 19501631]

Poyhia R, Kalso EA (1992) Antinociceptive effects and central nervous system depression caused by oxycodone and morphine in rats. Pharmacol Toxicol 70:125–130. [PubMed: 1508838]

Pradhan AA, Becker JA, Scherrer G, Tryoen-Toth P, Filliol D, Matifas A, Massotte D, Gaveriaux-Ruff C, Kieffer BL (2009) *In vivo* delta opioid receptor internalization controls behavioral effects of agonists. PLoS One 4:e5425. [PubMed: 19412545]

Ribeiro-Dasilva MC, Shinal RM, Glover T, Williams RS, Staud R, Riley JL, 3rd, Fillingim RB (2011) Evaluation of menstrual cycle effects on morphine and pentazocine analgesia. Pain 152:614–622. [PubMed: 21239109]

Rogers SA, Kempen TA, Pickel VM, Milner TA (2016) Enkephalin levels and the number of neuropeptide Y-containing interneurons in the hippocampus are decreased in female cannabinoid-receptor 1 knock-out mice. Neurosci Lett 620:97–103. [PubMed: 27012427]

Saland LC, Hastings CM, Abeyta A, Chavez JB (2005) Chronic ethanol modulates delta and mu-opioid receptor expression in rat cns: Immunohistochemical analysis with quantitiative confocal microscopy. Neurosci Lett 381:163–168. [PubMed: 15882810]

Scharfman HE, MacLusky NJ (2014) Sex differences in the neurobiology of epilepsy: A preclinical perspective. Neurobiol Dis 72 Pt B:180–192. [PubMed: 25058745]

Shenoy SK, Lefkowitz RJ (2011) Beta-arrestin-mediated receptor trafficking and signal transduction. Trends Pharmacol Sci 32:521–533. [PubMed: 21680031]

Soderberg Lofdal KC, Andersson ML, Gustafsson LL (2013) Cytochrome p450-mediated changes in oxycodone pharmacokinetics/pharmacodynamics and their clinical implications. Drugs 73:533–543. [PubMed: 23605691]

Sperk G, Hamilton T, Colmers WF (2007) Neuropeptide Y in the dentate gyrus. Prog Brain Res 163:285–297. [PubMed: 17765725]

Stumm RK, Zhou C, Schulz S, Hollt V (2004) Neuronal types expressing mu- and delta-opioid receptor mRNA in the rat hippocampal formation. J Comp Neurol 469:107–118. [PubMed: 14689476]

Swanson LW (1992) Brain maps: Structure of the rat brain, 1 Edition. Amsterdam: Elsevier.

Torres-Reveron A, Khalid S, Williams TJ, Waters EM, Drake CT, McEwen BS, Milner TA (2008) Ovarian steroids modulate leu-enkephalin levels and target leu-enkephalinergic profiles in the female hippocampal mossy fiber pathway. Brain Res 1232:70–84. [PubMed: 18691558]

Torres-Reveron A, Williams TJ, Chapleau JD, Waters EM, McEwen BS, Drake CT, Milner TA (2009a) Ovarian steroids alter mu opioid receptor trafficking in hippocampal parvalbumin gabaergic interneurons. Exp Neurol 219:319–327. [PubMed: 19505458]

Torres-Reveron A, Khalid S, Williams TJ, Waters EM, Jacome L, Luine VN, Drake CT, McEwen BS, Milner TA (2009b) Hippocampal dynorphin immunoreactivity increases in response to gonadal steroids and is positioned for direct modulation by ovarian steroid receptors. Neuroscience 159:204–216. [PubMed: 19150393]

Turner CD, Bagnara JT (1971) General endocrinology Philadelphia: W.B. Saunders.

Van Kempen TA, Gorecka J, Gonzalez AD, Soeda F, Milner TA, Waters EM (2014) Characterization of neural estrogen signaling and neurotrophic changes in the accelerated ovarian failure mouse model of menopause. Endocrinology 155:3610–3623. [PubMed: 24926825]

Van Kempen TA, Kahlid S, Gonzalez AD, Spencer-Segal JL, Tsuda MC, Ogawa S, McEwen BS, Waters EM, Milner TA (2013) Sex and estrogen receptor expression influence opioid peptide levels in the mouse hippocampal mossy fiber pathway. Neurosci Lett 552:66–70. [PubMed: 23933204]

Van Kempen TA, Dodos M, Woods C, Marques-Lopes J, Justice NJ, Iadecola C, Pickel VM, Glass MJ, Milner TA (2015) Sex differences in NMDA gluN1 plasticity in rostral ventrolateral medulla neurons containing corticotropin-releasing factor type 1 receptor following slow-pressor angiotensin II hypertension. Neuroscience 307:83–97. [PubMed: 26306872]

Volkow ND, Wang GJ, Telang F, Fowler JS, Logan J, Childress AR, Jayne M, Ma Y, Wong C (2006) Cocaine cues and dopamine in dorsal striatum: Mechanism of craving in cocaine addiction. J Neurosci 26:6583–6588. [PubMed: 16775146]

Walker QD, Nelson CJ, Smith D, Kuhn CM (2002) Vaginal lavage attenuates cocaine-stimulated activity and establishes place preference in rats. Pharmacol Biochem Behav 73:743–752. [PubMed: 12213518]

Walker QD, Cabassa J, Kaplan KA, Li ST, Haroon J, Spohr HA, Kuhn CM (2001) Sex differences in cocaine-stimulated motor behavior: Disparate effects of gonadectomy. Neuropsychopharmacology 25:118–130. [PubMed: 11377925]

Williams TJ, Milner TA (2011) Delta opioid receptors colocalize with corticotropin releasing factor in hippocampal interneurons. Neuroscience 179:9–22. [PubMed: 21277946]

Williams TJ, Torres-Reveron A, Chapleau JD, Milner TA (2011a) Hormonal regulation of delta opioid receptor immunoreactivity in interneurons and pyramidal cells in the rat hippocampus. Neurobiol Learn Mem 95:206–220. [PubMed: 21224009]

Williams TJ, Akama KT, Knudsen MG, McEwen BS, Milner TA (2011b) Ovarian hormones influence corticotropin releasing factor receptor colocalization with delta opioid receptors in ca1 pyramidal cell dendrites. Exp Neurol 230:186–196. [PubMed: 21549703]

Wissman AM, May RM, Woolley CS (2012) Ultrastructural analysis of sex differences in nucleus accumbens synaptic connectivity. Brain Struct Funct 217:181–190. [PubMed: 21987050]

Wong M, Moss RL (1992) Long-term and short-term electrophysiological effects of estrogen on the synaptic properties of hippocampal CA1 neurons. J Neurosci 12:3217–3225. [PubMed: 1353794]

Zhang Y, Windisch K, Altschuler J, Rahm S, Butelman ER, Kreek MJ (2016) Adolescent oxycodone self administration alters subsequent oxycodone-induced conditioned place preference and anti-nociceptive effect in C57BL/6J mice in adulthood. Neuropharmacology 111:314–322. [PubMed: 27614221]

Znamensky V, Akama KT, McEwen BS, Milner TA (2003) Estrogen levels regulate the subcellular distribution of phosphorylated AKT in hippocampal ca1 dendrites. J. Neurosci 23:2340–2347. [PubMed: 12657693]

Highlights

- The hippocampal opioid system has sex-specific changes following oxycodone (OXY) conditioned place preference (CPP).
- After OXY CPP, mossy fibers with Leu-Enkephalin rearrange differently in males and females to enhance opioid sensitivity.
- Delta opioid receptors (DORs) redistribute to mossy fiber-CA3 synapses in OXY CPP males in a manner resembling females.
- DORs and mu opioid receptors traffic in GABAergic interneurons in OXY CPP females in a way that would enhance disinhibition
- These sex-dependent changes in hippocampal opioid circuits may facilitate drug-associative learning particularly in females.

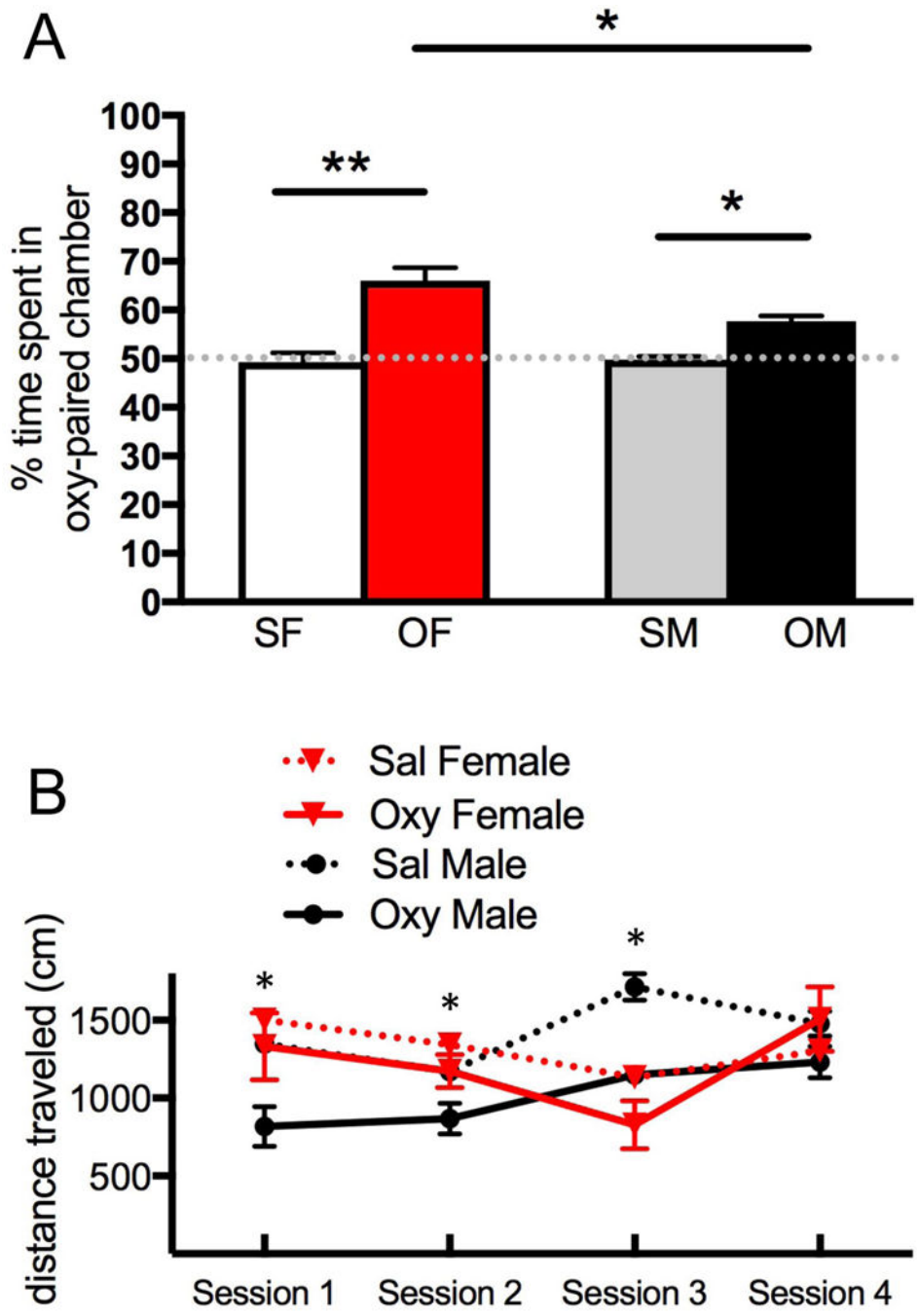

Fig. 1. Both female and rats develop oxycodone conditioned place preference (CPP).

A. During the preconditioning phase, female rats displayed a preference for the black side of the CPP chamber while males preferred the white side. Thus, a biased CPP design was used in which oxycodone was administered in the least-preferred side for that sex. On the testing day, Sal-female and Sal-male rats showed no preference for either chamber. However, the percent of time spent in the oxycodone-injected chamber is higher for both female (***$p<0.001$) and male (*$p<0.05$) rats compared to their saline-injected counterparts. Females spent significantly more time on the oxycodone-paired side than did the males (*p

<0.05). **B.** Locomotion scores for females and males for the oxycodone injection days during the four conditioning sessions and in the final test session for the CPP. Repeated measured ANOVA revealed that locomotion significantly increased in oxycodone-injected males (*p = 0.0103) but not in oxycodone-injected females during the first three training sessions. However, no significant differences in locomotion were found in either sex in the fourth oxycodone training session. N = 5–6 rats per group.

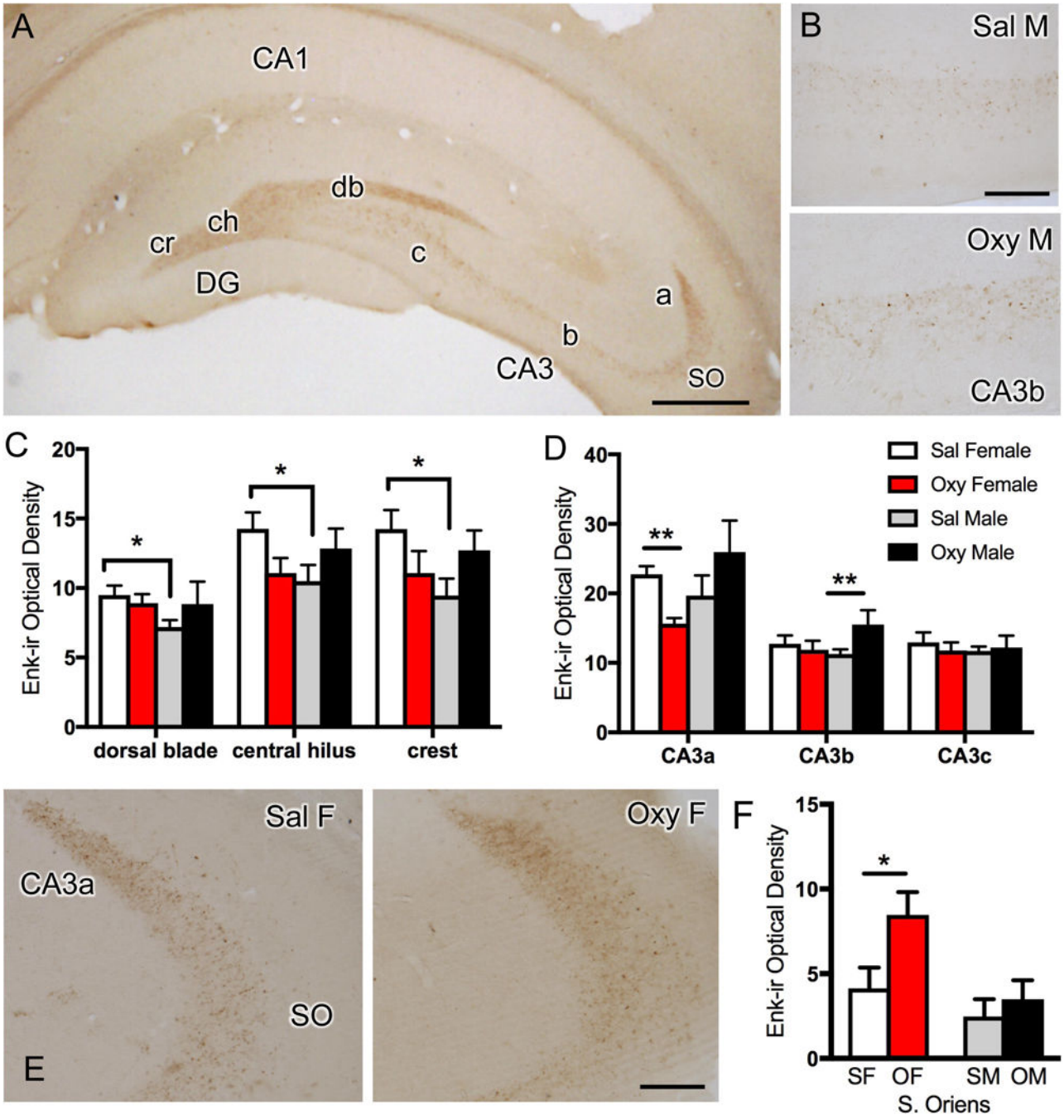

Fig. 2. Effects of oxycodone conditioned place preference (CPP) on the levels of Leu-Enkephalin-immunoreactivity (LEnk-ir) in the mossy fiber pathway.

A. Low magnification photomicrograph of the rat dorsal hippocampus shows LEnk-ir in the mossy fiber pathway within stratum lucidum of CA3a,b and c and in the crest (cr), central hilus (ch), and dorsal blade (db) of the dentate gyrus (DG). The region of CA3 stratum oriens (SO) sampled is also indicated. **B.** High magnification photomicrograph of LEnk-ir in stratum lucidum of CA3b in Sal-male and Oxy-male rats. **C.** Sal-females (estrus) compared to Sal-males have higher levels of LEnk-ir in the dorsal blade, central hilus and crest of the

DG. **D.** Oxy-females compared to Sal-females demonstrate decreased levels of LEnk-ir in CA3a. Oxy-males compared to Sal-males show significantly increased levels of LEnk-ir in the CA3b. **E.** High magnification photomicrograph of CA3a shows greater LEnk-ir levels in stratum lucidum in a Sal-female compared to an Oxy-female. However, greater densities of LEnk-ir are detected in SO of Oxy-females compared to Sal-females. **F.** Oxy-females (OF) compared to Sal-females (SF) have an increased density of LEnk-labeled mossy fibers in SO of CA3. SM = saline males; OM = Oxy males **$p < 0.01$, *$p < 0.05$; N = 5–6 rats per group. Scale bars: A, 500 μm; B & E = 100 μm

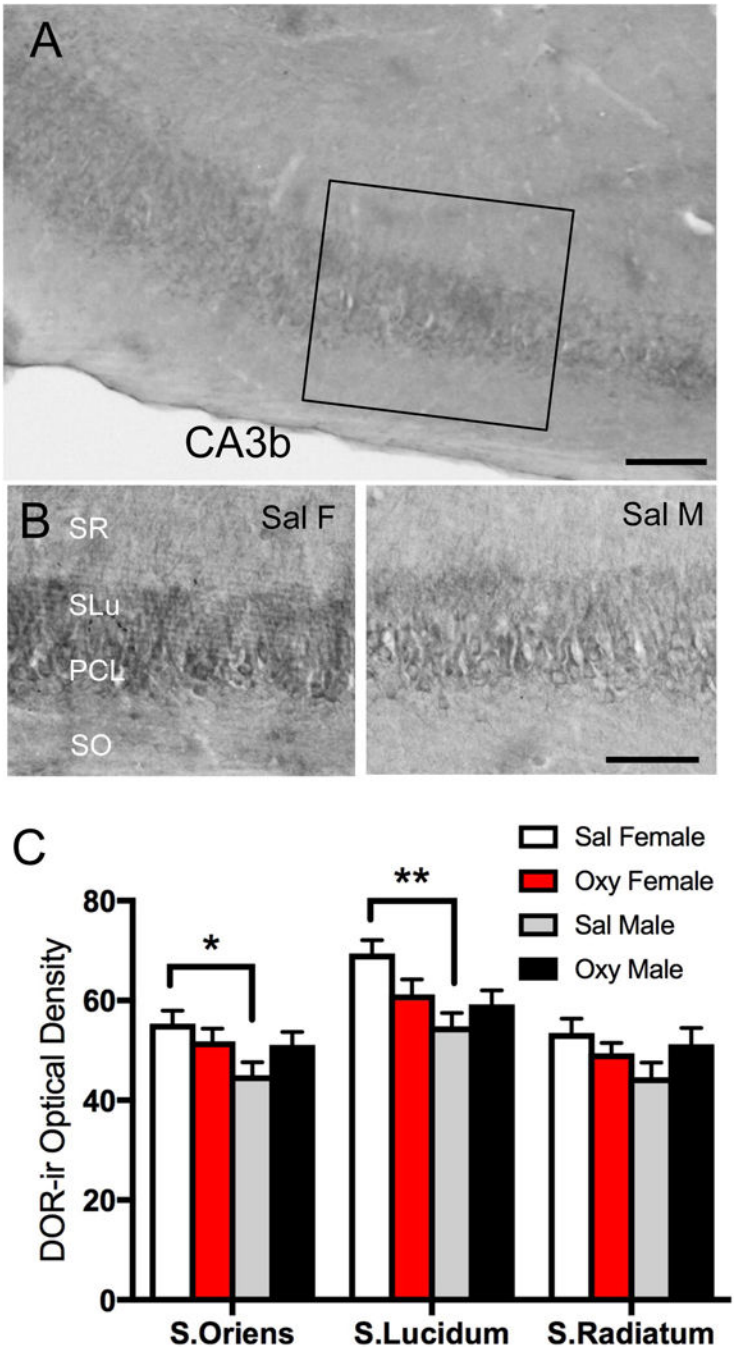

Fig. 3. Effects of oxycodone conditioned place preference (CPP) on the levels of delta opioid receptor-immunoreactivity (DOR-ir) in the CA3b region.

A. Low magnification photomicrograph shows DOR-ir in the CA3 region of the dorsal hippocampus; box indicates area of CA3b sampled for densitometry and EM studies. DG = dentate gyrus. **B.** Representative high magnification photomicrographs of stratum oriens (SO), pyramidal cell layer (PCL), stratum lucidum (SLu), and stratum radiatum (SR) of CA3b from a Sal-female (Sal F),and a Sal-male (Sal M). **C.** Sal-females compared to Sal-

males show significantly greater DOR-ir levels in stratum oriens and stratum lucidum of CA3b. Scale bars: A = 100 μm **p < 0.01, *p < 0.05; N = 6 rats per group).

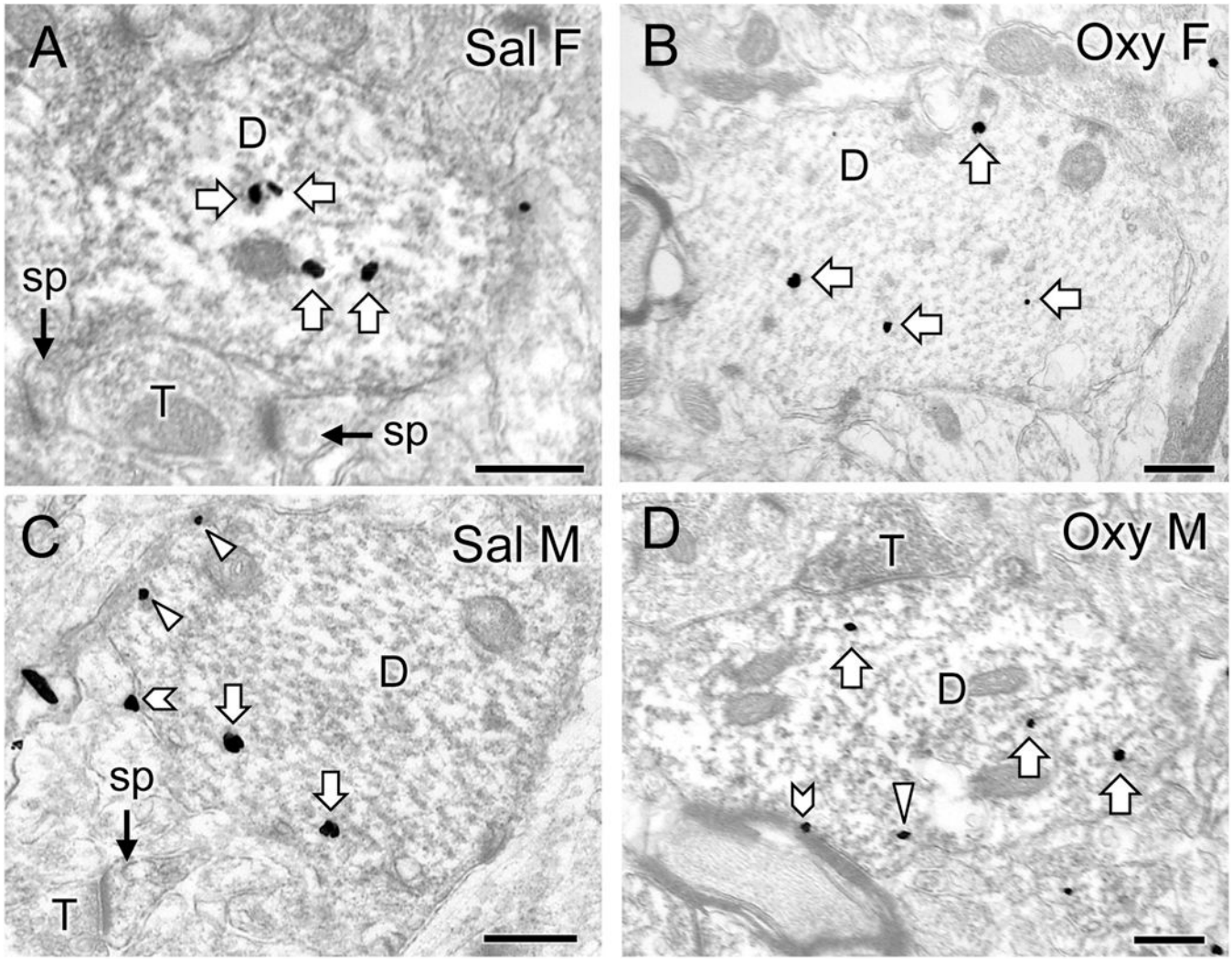

Fig. 4. Representative electron micrographs of delta opioid receptor (DOR) silver-intensified gold (SIG) particles in CA3 pyramidal cell dendrites from saline-injected and oxycodone conditioned place preference rats.

A-D. Electron micrographs show the distribution of DOR-SIG particles within CA3 pyramidal cell dendrites from a Sal-female (**A**), an Oxy-female (**B**), a Sal-male (**C**), and an Oxy-male (**D**). Examples of on the plasmalemma (chevron), near the plasmalemma (triangle) and cytoplasmic (white arrow) DOR-SIG particles in dendrites are shown. CA3 dendrites often have spines (sp) that are contacted by terminals (T). The Oxy-female has a higher density of DOR-SIG particles in total in CA3 pyramidal dendrites compared to the Sal-female. The Oxy-male has fewer near plasmalemmal DOR-SIG particles in CA3 pyramidal dendrites compared to the Sal-male. Scale bar: 500 nm.

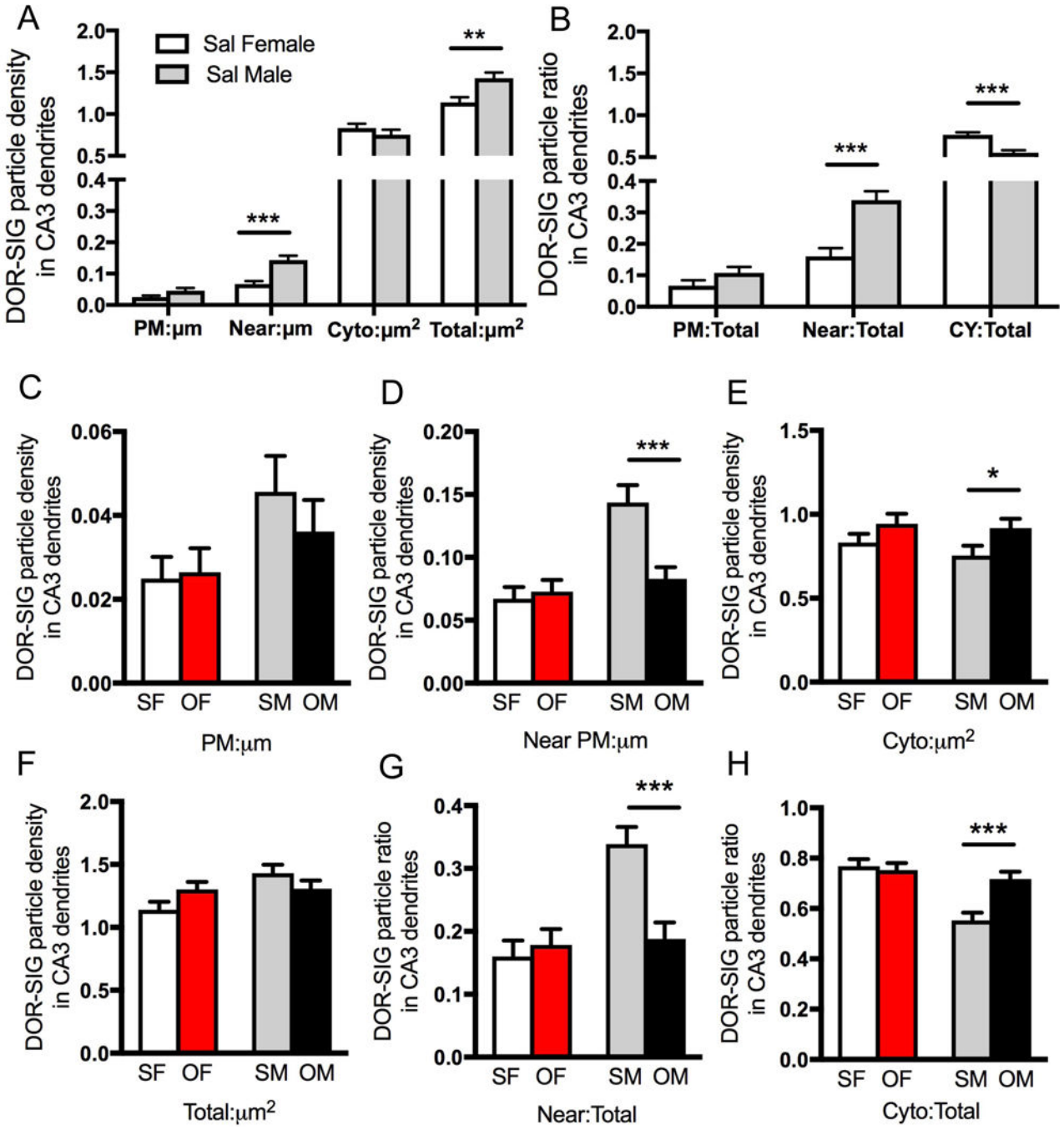

Fig 5. Sex differences in the distribution of delta opioid receptor (DOR) silver-intensified gold (SIG) particles in CA3 pyramidal cell dendrites in saline-injected and oxycodone conditioned place preference rats.

A. Sal-females have a significantly lower density of DOR-SIG particles on the plasmalemma, near the plasmalemma and in total in CA3 pyramidal cell dendrites compared to saline-injected males. **B.** Compared to saline-injected males, the partitioning ratio of DOR-SIG particles in CA3 dendrites is significantly lower near the plasmalemma and higher in the cytoplasm of saline-injected females. **C-H.** Sal- and Oxy-females (SF & OF, respectively) have no changes in either the density or partitioning ratio of DOR-SIG

particles in any compartment in CA3 dendrites. Compared to Sal-males (SM), Oxy-males (OM) show a decrease in the density and partitioning ratio of DOR-SIG particles near the plasmalemma (**D, G**) and an increase in the partitioning ratio of DOR-SIG particles in the cytoplasm of CA3 dendrites (**H**). ***$p < 0.001$, **$p < 0.01$, *$p < 0.05$; N = 3 rats per group; n = 50 dendrites per rat.

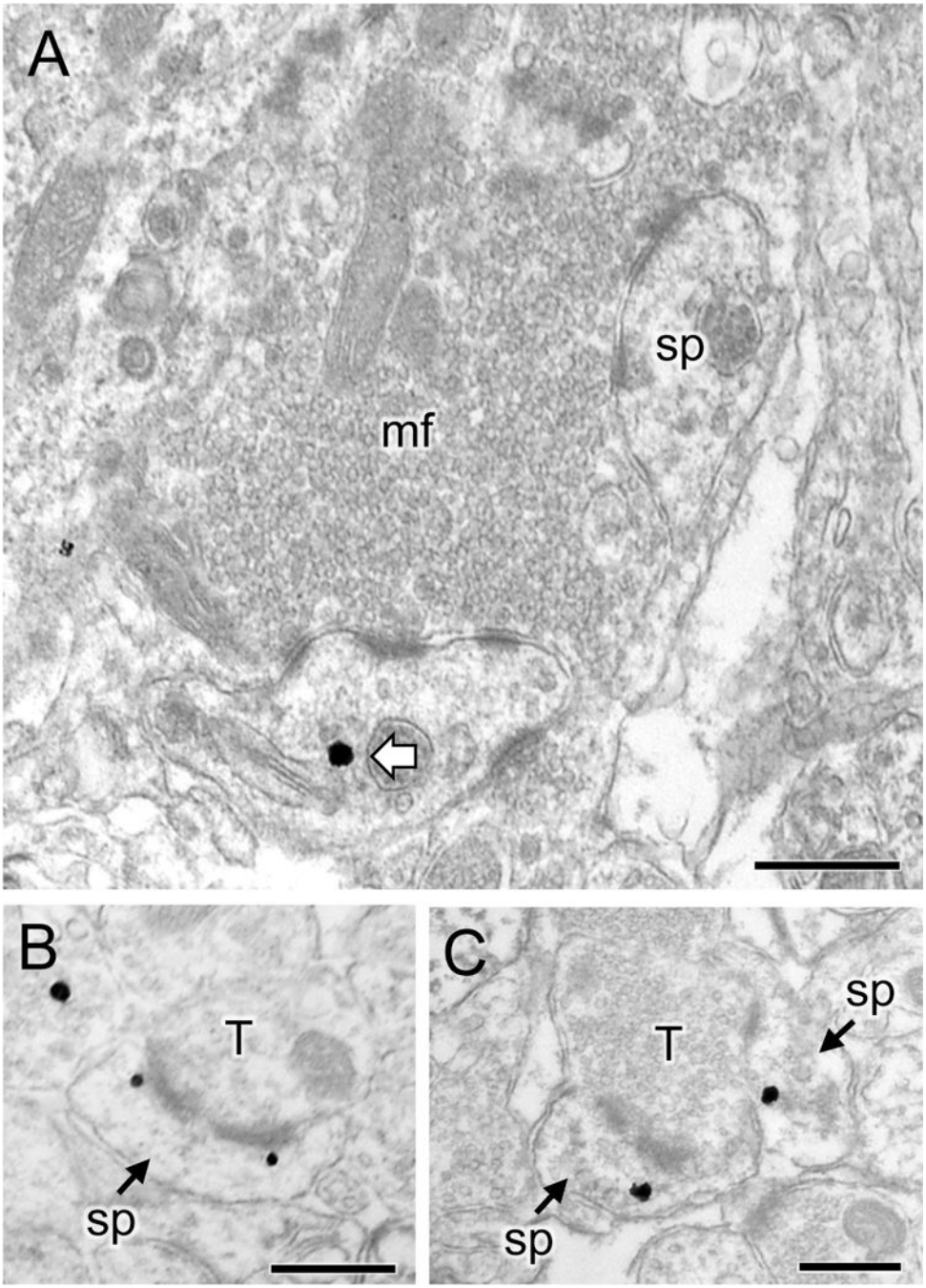

Fig 6. Representative micrographs of delta opioid receptor (DOR)-labeled dendritic spines in CA3.

A. Representative electron micrograph from stratum lucidum of CA3 of an Oxy-male rat shows a DOR silver-intensified gold (SIG) particle in the cytoplasm of a dendritic spine (sp) in contact with a mossy fiber (mf) in the CA3. **B, C.** Representative electron micrographs from stratum radiatum of CA3 of an Oxy-female rat show DOR-SIG particles near the perforated synapse (**B**) or in the cytoplasm (**C**) of two dendritic spines (sp) which are contacted by a terminal (T). Scale bar: 500 nm.

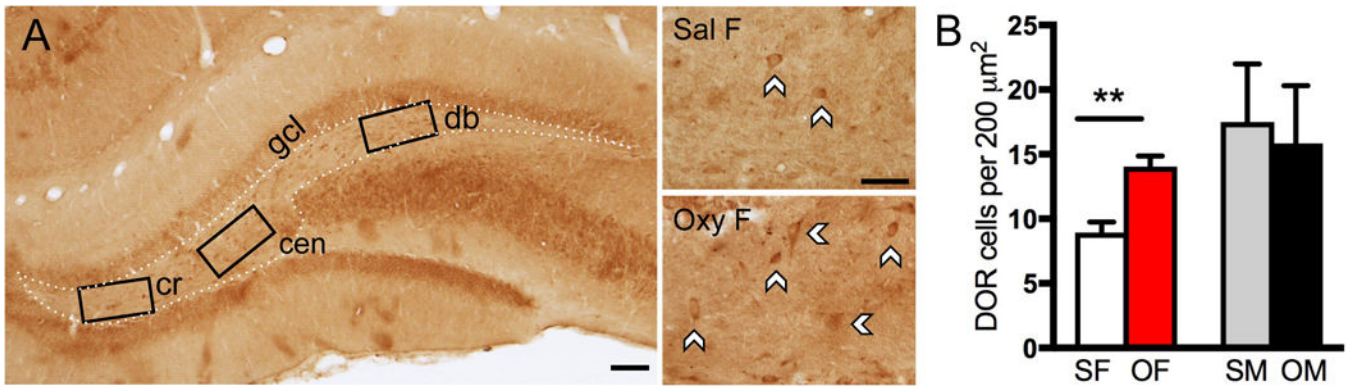

Fig. 7. The number of delta opioid receptor (DOR)-labeled cells in the hilus of the dentate gyrus is altered in females following oxycodone conditioned place preference.

A. Low magnification photomicrograph shows DOR-containing cells in three regions of the hilus (cr = crest; cen = central hilus; db = dorsal blade). Representative high magnification photomicrographs (right) of the central hilus show a greater number of labeled cells in the Oxy-female compared to the Sal-female. Scale bar: 100 µm (left); 50 µm (right). **B.** Compared to Sal-females, Oxy-females show an increased number of DOR cells in the central hilus (**$p < 0.01$).

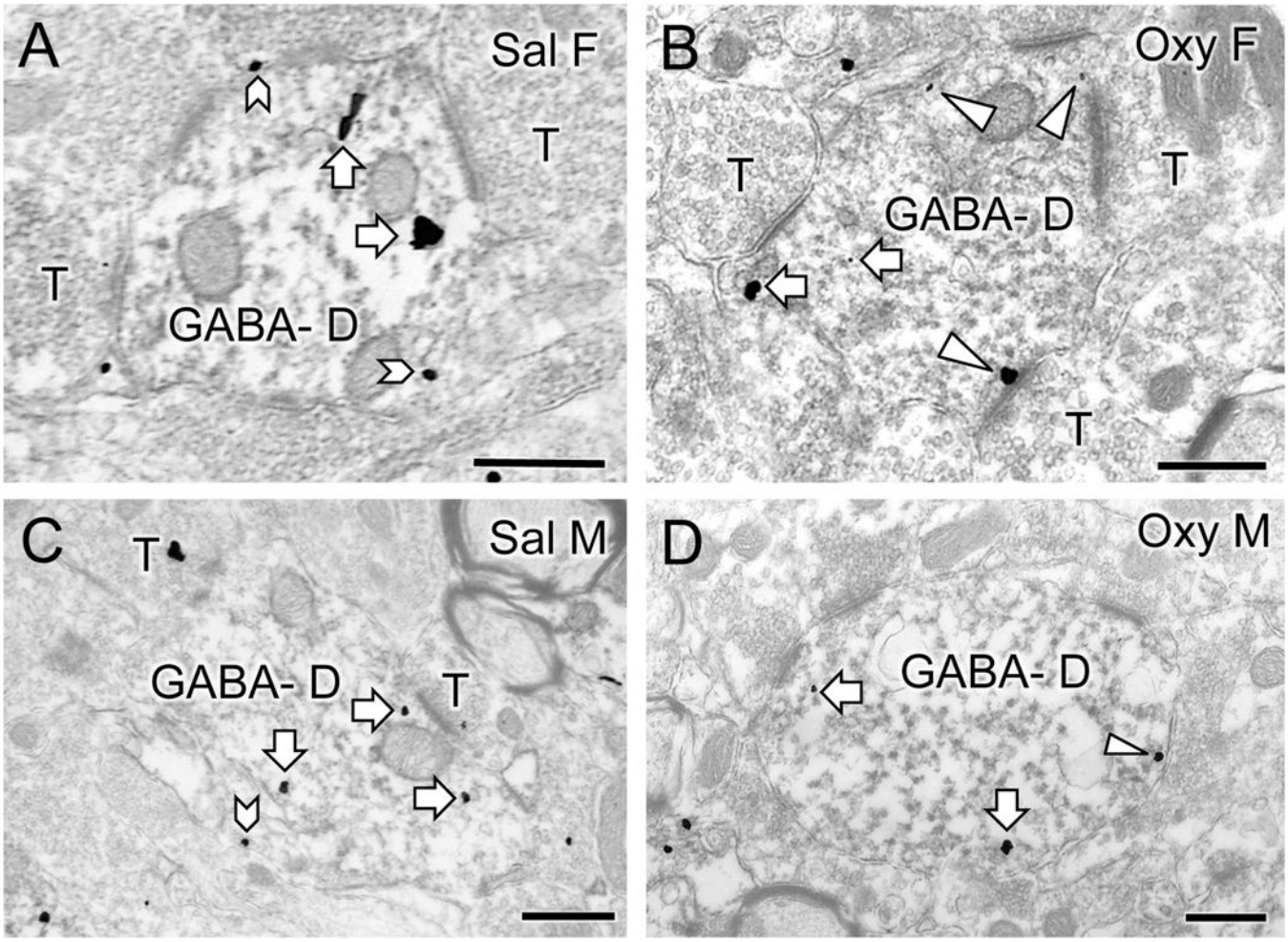

Fig. 8. Representative electron micrographs of delta opioid receptor (DOR) silver-intensified gold (SIG) particles in GABAergic hilar dendrites from saline-injected and oxycodone condition place preference rats.

A-D. Electron micrographs show the distribution of DOR-SIG particles within GABA-labeled dendrites (GABA-D) in the hilus from a Sal-female (**A**), an Oxy-female (**B**), a Sal-male (**C**) and an Oxy-male (**D**). Examples of on the plasmalemma (chevron), near plasmalemmal (triangle) and cytoplasmic (white arrow) DOR-SIG particles in dendrites are shown. The saline-injected female compared to saline-injected male has more plasmalemmal DOR-SIG particles in the GABA-labeled dendrite. The Oxy-female compared to the Sal-female has more DOR-SIG particles near the plasmalemma of the GABA-labeled dendrite. The Oxy-male compared to the Sal-male exhibits a decrease in the cytoplasmic density of DOR-SIG labeling in the GABA-labeled dendrite. Scale bar: 500 nm.

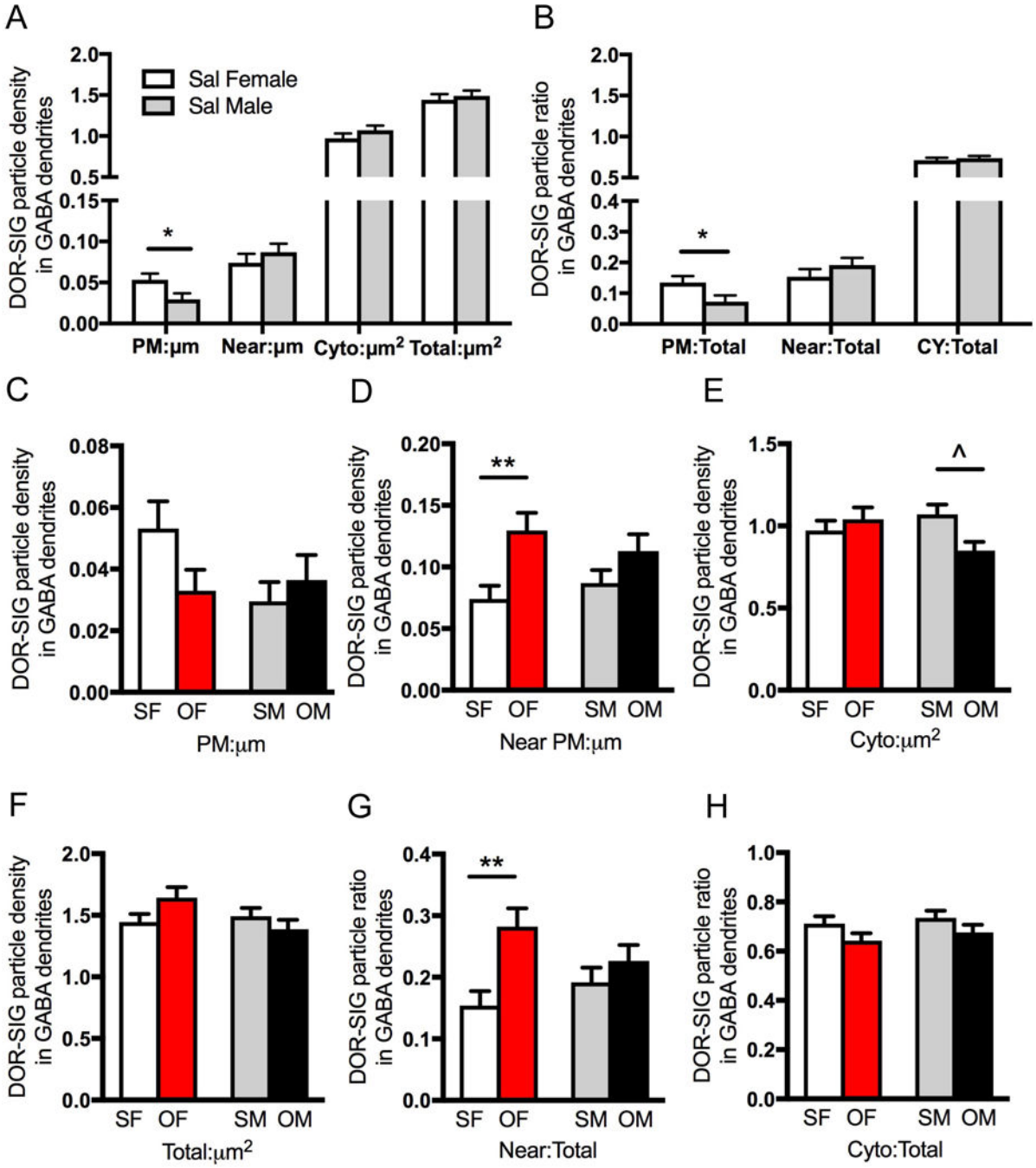

Fig. 9. Sex differences in the distribution of delta opioid receptor (DOR) silver-intensified gold (SIG) particles in GABAergic hilar dendrites in saline-injected and oxycodone condition place preference rats.

A. Sal-females compared to Sal-males have a greater density of DOR-SIG particles on the plasmalemma (PM) in GABA-labeled dendrites. **B.** The partitioning ratio for DOR-SIG particles is increased near the plasmalemma (Near) in GABA-labeled dendrites in Sal-females compared to Sal-males. **C-H.** Density and partitioning ratios of DOR-SIG particles in subcellular compartments of GABA-labeled dendrites are shown. Oxy-females (OF) compared to Sal-females (SF) show increased density and partitioning ratio of DOR-SIG

particles near the plasmalemma in GABA-labeled dendrites (**D & H**). Oxy-males (OM) compared to Sal-males (SM) show a decrease in DOR-SIG particle density in the cytoplasm of GABA-labeled dendrites (**E**). **$p < 0.01$, *$p \leq 0.05$. N = 3 rats per group; n = 50 dendrites per rat.

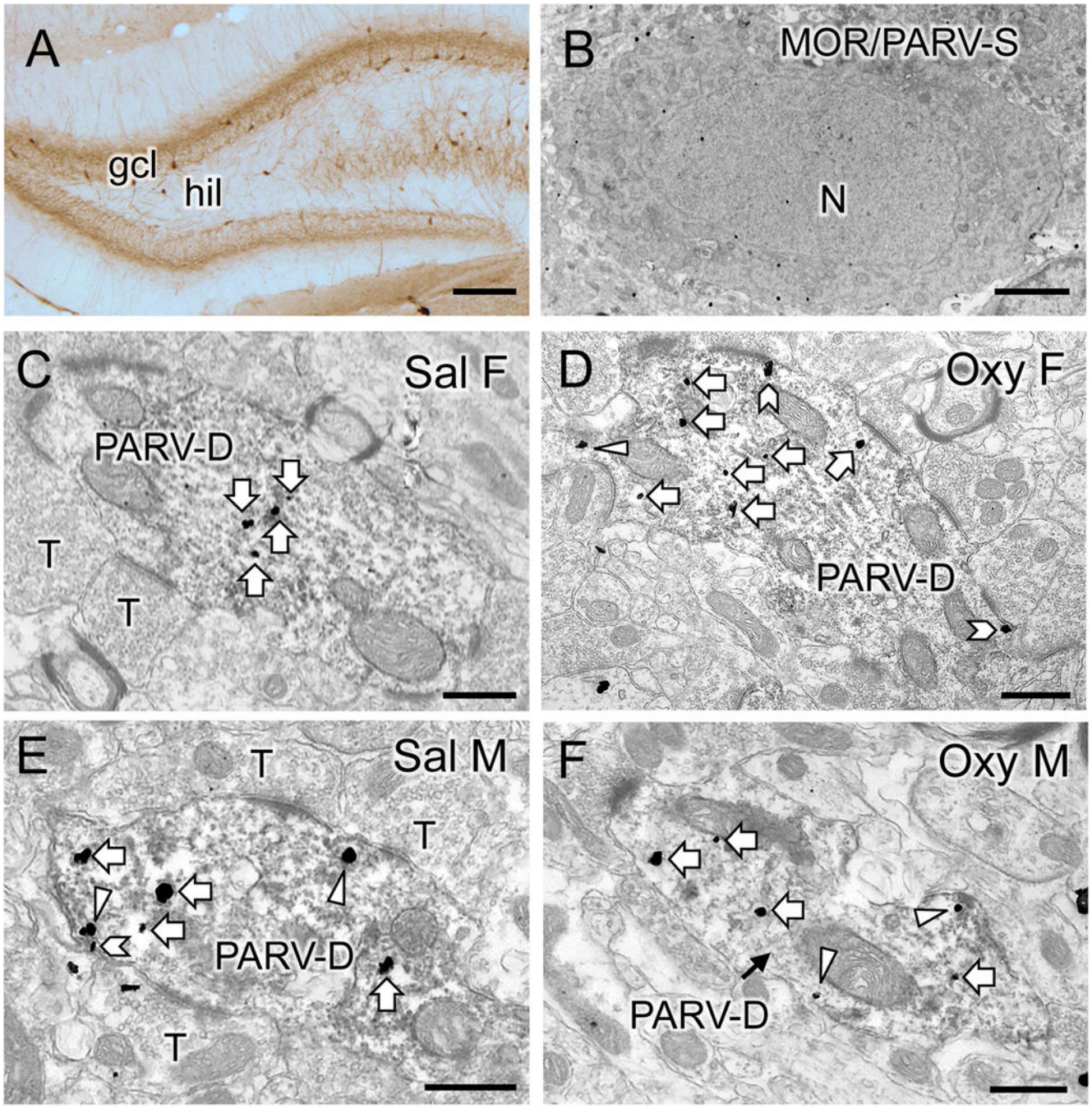

Fig. 10. Representative electron micrographs of mu opioid receptor (MOR) silver intensified gold (SIG) particles in parvalbumin (PARV)-containing interneurons in the dentate gyrus.

A. Low magnification photomicrograph shows PARV-labeled cells are primarily located in the subgranular region of the hilus (hil) in the dentate gyrus (gcl = granule cell layer). **B.** Example of somata in the subgranular zone of the hilus dually labeled for MOR-SIG particles and PARV (immunoperoxidase). N, nucleus. **C-F.** Representative micrographs show the distribution of MOR-SIG particles within peroxidase-labeled PARV dendrites in the dentate gyrus for a Sal-female (**C**), an Oxy-female (**D**), a Sal-male (**E**), and an Oxy-male

(**D**). Examples of on the plasmalemma (chevron), near the plasmalemma (triangle) and cytoplasmic (white arrow) MOR-SIG particles in dendrites are shown. Saline-injected females showed a lower overall density of MOR-SIG particles in PARV-labeled dendrites relative to saline-injected males, but after oxycodone CPP the density of plasmalemmal and total of MOR-SIG particles increased in PARV-labeled dendrites in females only. Scale bars: A = 500 μm; B, C-F = 500 nm.

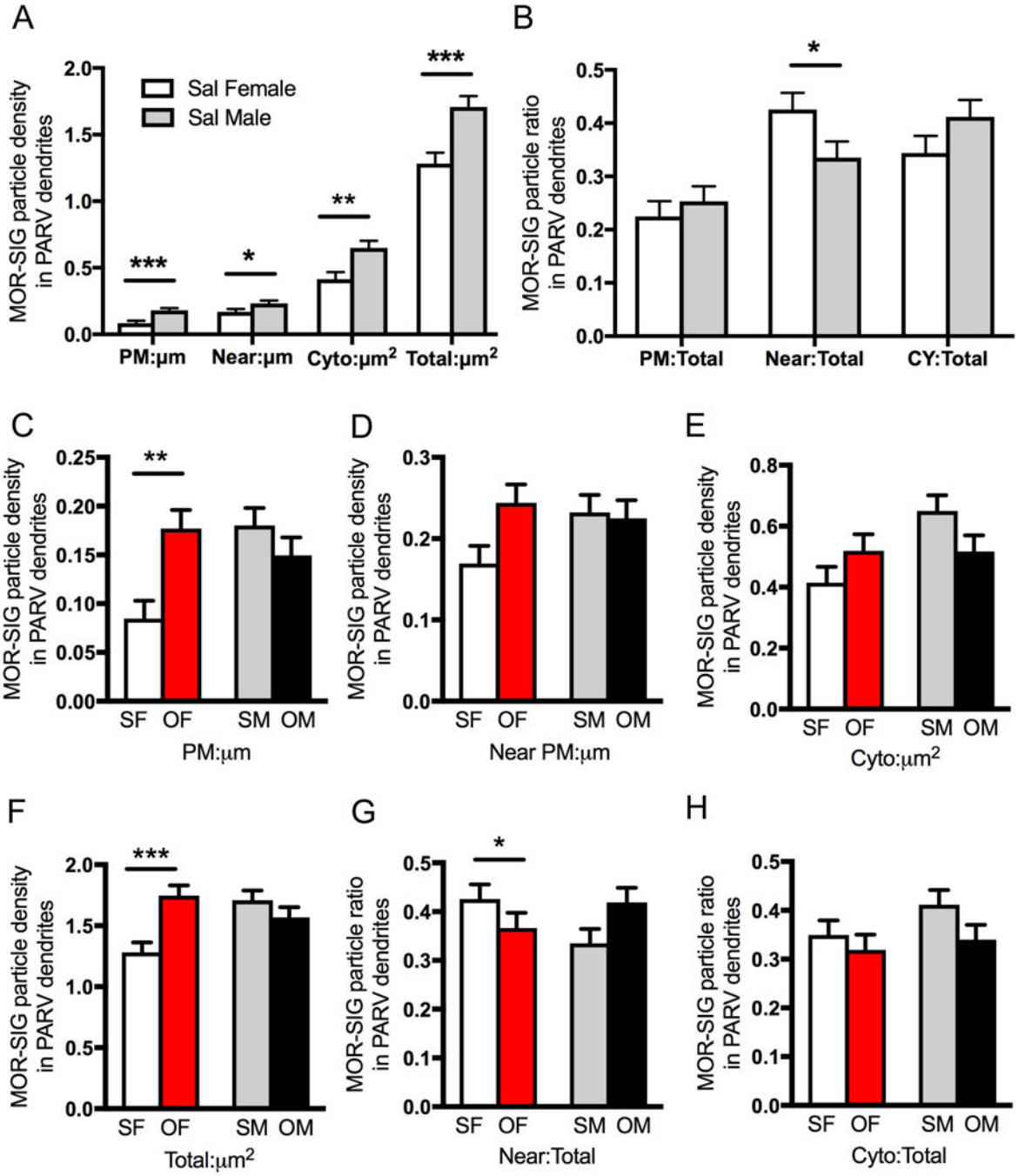

Fig. 11. Sex differences in the distribution of mu opioid receptor (MOR) silver-intensified gold (SIG) particles in hilar parvalbumin (PARV)-labeled interneurons in saline-injected and oxycodone condition place preference rats.

A. Sal-females compared to Sal-males have lower densities of MOR-SIG particles localized on the plasmalemma (PM), near the plasmalemma (Near), in the cytoplasm (Cyto), and in total in PARV-labeled dendrites. **B.** Sal-females compared to Sal-males have a significantly larger proportion of MOR-SIG particles near the plasmalemma of PARV-labeled dendrites. **C-H.** Density and partitioning ratios of MOR-SIG particles in the subcellular compartments of PARV-labeled dendrites are shown. Compared to Sal-females (SF), Oxy-females (OF)

showed a significant increase in MOR-SIG particle density on the plasmalemma (**C**) and in total (**F**) within PARV-labeled dendrites. No differences in the partitioning ratio of MOR-SIG particles in PARV-labeled dendrites were seen in Oxy- and Sal-females. No differences in either the density or the partitioning ratio of MOR-SIG particles in PARV-labeled dendrites were seen in Sal- and Oxy-males. ***$p < 0.001$, **$p < 0.01$, *$p < 0.05$; N = 3 rats per group; n = 50 dendrites per rat.

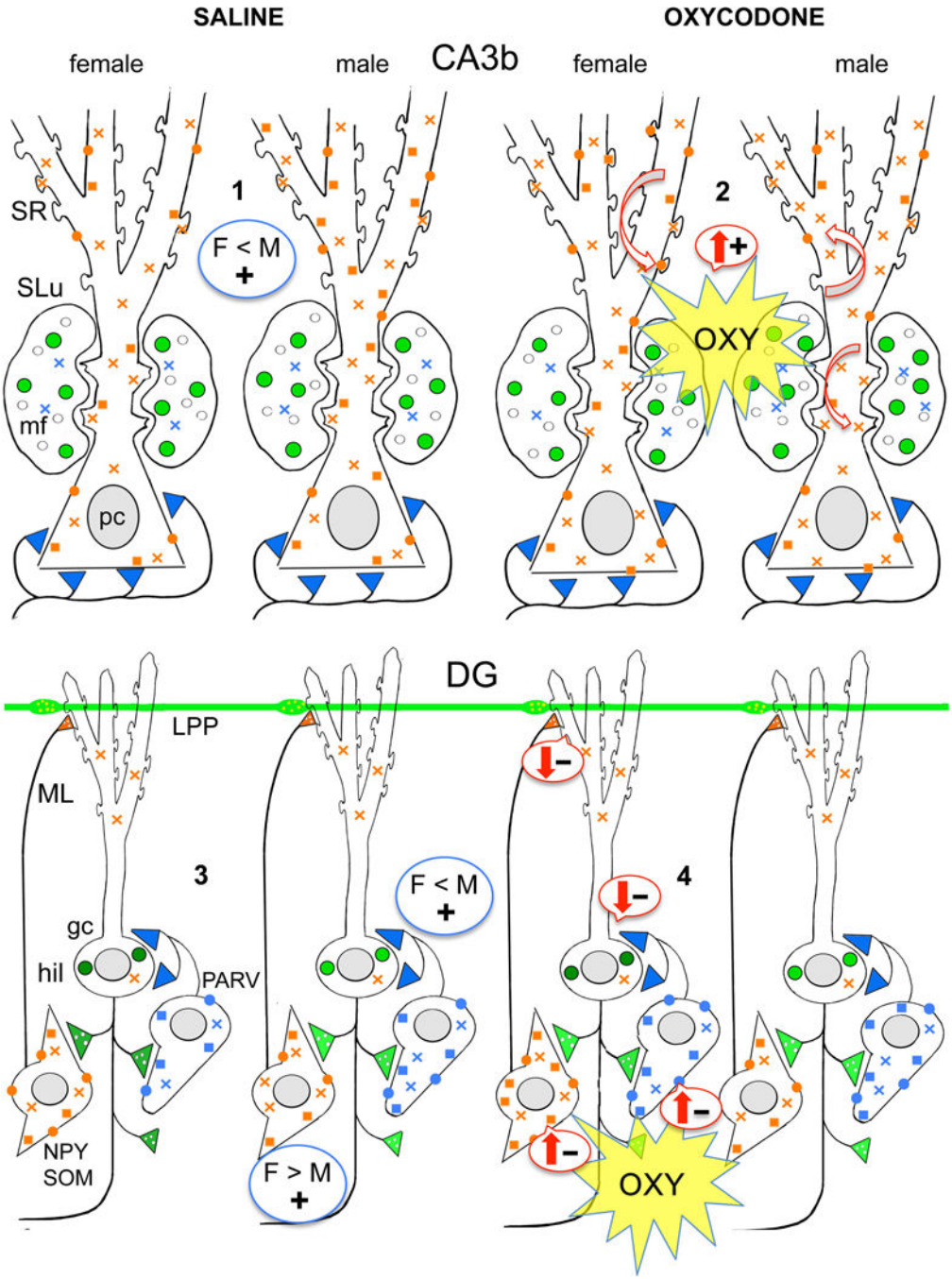

Fig. 12. Schematic illustrating sex differences in the hippocampal opioid system in saline-injected (control) and oxycodone condition place preference (CPP) rats.

Red arrows indicate predicted effects of delta opioid receptor (DOR) and mu opioid receptor (MOR) trafficking changes on excitation (plus signs) and inhibition (minus signs) in the CA3 and dentate gyrus (DG). **#1–4** indicate points where there are differences in the distribution of DORs and MORs in saline-injected and oxycodone CPP rats. gc, granule cell; hil, hilus; lpp, lateral perforant path; ML, molecular layer; mf, mossy fiber; SLu, stratum lucidum; SR, stratum radiatum. Blue color = MORs; Green color = Leu-Enkephalin (LEnk)

levels; orange color = DORs. Circles = plasmalemmal receptors; squares = near-plasmalemmal receptors; crosses = cytoplasmic receptors.

1. Sal-females compared to Sal-males have fewer near-plasmalemmal and total DORs in SR CA3 pyramidal cell dendrites.

2. Oxy-females compared to Sal-females have more DORs in the spines of SR CA3 dendrites. Oxy-males compared to Sal-males have fewer near plasmalemmal DORs in SR CA3 dendrites and more DORs in the spines of CA3 pyramidal cells contacted by mossy fibers. Oxy-males compared to Sal-males also have greater LEnk levels in mossy fibers.

3. Sal-females compared to Sal-males have elevated plasmalemmal DORs on the dendrites of GABAergic-labeled interneurons previously shown to colocalize somatostatin and neuropeptide Y (Commons and Milner, 1996; Williams and Milner, 2011). Sal-females compared to Sal-males have fewer plasmalemmal MORs on the dendrites of parvalbumin (PARV)-containing interneurons.

4. In Oxy-females, near-plasmalemmal DORs increase in GABA-labeled dendrites and plasmalemmal and total MORs increase in PARV-labeled dendrites. Moreover, the number of DOR-immunoreactive hilar interneurons is increased in Oxy-females compared to Sal-females.

Table 1.

DOR-labeled spines in CA3

Group	% ± SEM labeled spines	# ± SEM labeled spines	Location		
			synapse	membrane	cytoplasm
Stratum Lucidum					
Sal Male	9.5 ± 1.8	11.7 ± 1.8	3	16	16
Oxy Male	12.5 ± 2.8	13.7 ± 2.3	4	14	33
Sal Female	8.0 ± 1.5	9.0 ± 1.0	4	5	18
Oxy Female	10.6 ± 4.4	12 ± 3.6	6	11	19
Stratum Radiatum					
Sal Male		9.0 ± 2.0	0	13	16
Oxy Male		6.3 ± 1.67	2	7	12
Sal Female		4.0 ± 0.58	0	4	9
Oxy Female		10.3 ± 2.4	5	14	17

*Some spines had more than one DOR-SIG particle. Stratum lucidum: percentage of spines determined from dendritic spines contacted by 50 randomly selected mossy fiber terminals per rat. Stratum radiatum: 100 dendritic spines were selected randomly from the micrographs. N = 3 rats per condition